SCHOOL OF ENGINEERING
MSc(Eng)

TOROIDAL SHELLS SUBJECTED TO EXTERNAL PRESSURES

DISSERTATION REPORT

Baris Akin

Student Number: 200893695
Aerospace and Mechanical Systems Engineering

Sep 2013

Supervisor: Dr.Blachut

School of Engineering
The University of Liverpool
Brownlow Hill, LIVERPOOL, L69 3GH

Summary

The toroidal shell applications are becoming more common for both vessel and hull technologies. The purpose of this research is to offer and discuss different configurations of toroidal shells which will be subjected to external pressure. It also shows the importance of using toroidal shells as pressure hulls, for underwater or aeronautical applications. This paper also discusses the importance and dependency of imperfections on the toroidal shells. This paper studies different toroidal shell configurations from theoretical, experimental and numerical approach for external pressures.

Table of Contents

Table of Figures

List of Tables

Table of Notations

		Unit
A	Rate of hardening	N/m^2
a	Radius of toroid subtracted from the radius of cross-sectional circle	m
a_0	Initial value of a	m
B	Measure of initial state of the material	-
b	Mode of deflection multiplier	-
D	Bending stiffness	N/m
E	Young's modulus of elasticity	Pa
h	Shell thickness	m
J	Moment of inertia	kg.m^2
K	Buckling parameter	-
K	The ratio of height to width for an ellipse	-
k_1	The ratio of torsional stiffness to bending stiffness	-
k_2	The ratio of torsional torque to bending stiffness multiplied by R	-
l	The height of Hutchinson's model	m
n	Measure of increment of rate hardening	-
P_0	Uniform normal pressure	N
ρ	Density of the material	kg/m^3
R	Radius of toroid	m
R_0	Initial value of toroid's radius	m
r	Radius of cross-sectional circle	m
r_0	Initial value of r	m
r_x	The distance between the curve's centre and curve surface	m
r_y	The distance between the centre of the shell and the curve	m

$u(\omega)$	Roll motion speed	rad/s
V	Auxiliary function	-
v	Poisson’s ratio	-
ω_{nm}	The mth root of the characteristic of the equation	-
x	Ratio of meridional stress to circumferential stress	-
$y(\psi, t)$	Out-of plane bending displacement	m
Z	Length parameter	-
z_{nm}	The mth root of moment of intertia	kg/m^3
z	Subtangent of a shell	m
α	Ratio of radius of toroid and cross-sectional circle’s radius	-
θ	Torsional angle of toroid	rad
$\phi(\psi, t)$	Torsional displacement	rad
$\bar{\varepsilon}$	Mode of deflection	-
σ	Mass per unit length of toroid	N/m^2
λ	Load	N

1. Introduction

1.1 Background

The toroidal shells are a very special form of geometry which is being used for various kinds of needs of needs in industrial applications due to its advantages of its mechanical properties. They are mostly used for to contain high-pressurized fluid (Redekop et al. 1999)however; it is also being used in various applications like propulsive devices (Shikhirin 2013), therefore it is important to understand the characteristics of toroidal shells. Considering its mechanical advantages, toroidal shells are being considered or used in underwater applications such as “missile launchers compromising of large toroidal shells” (Sun cited in Ross 2010) or “underwater toroidal pressure hulls” (Sun cited in Blachut 2010). For underwater toroidal shell usage conditions or for other applications which the toroid may be externally pressurised, it is important to understand the toroidal shell’s behaviour. Blachut (2004) suggests that, using toroidal shells for sub water vehicles, to obtain a more rigid pressure hull. Moreover, by changing the cross sectional geometry of toroidal shell, from circular to elliptical for semi axis condition a/b>1.0 buckling pressures can be considerably increased, although men has reached maximum depth of 6 km. underwater with an underwater vehicle.

For underwater applications Italian defence company, Maritalia already designed a submarine using toroids as a hull (Galletly 2000). The hull also works as storage for liquid oxygen which is 350 higher than the atmospheric pressure and it operates with a closed-cycle diesel engine (Ibid). One of the advantages of this configuration is that, it cannot be detected easily because of this system (Ibid).

Another usage of underwater toroidal shells can be drill systems. Ross has proposed an offshore drilling system with a toroidal shell hull for deep drilling missions (Galletly 2000). For international thermonuclear reactor (ITER) projects the toroidal shells are being considered to be used (Ibid). Moreover, Japanese investors have published a paper on the use of toroidal shells for aerospace applications (Ibid). Toroidal shells are becoming more important part in the industry. This is why, it is important to understand the behaviour of toroidal shells under different conditions to use on various applications.

1.2 Aims and Objectives

The purpose of this project is to evaluate the behaviour of toroidal shells’ buckling under different external horizontal loadings. To investigate the buckling of toroidal shells under different external loadings, computational simulation and experimental tests will be presented and the significance of the results will be discussed. To understand the elastic limits of toroidal shell experiments and computational analysis will be made by using ABAQUS software to validate the results. The research will carry on exploring the plastic deformation of toroidal shell. This project aims to carry out Michael Ross's (2013) project and identify his MRT2-2 toroidal shell's behaviour under higher horizontal loadings. The objectives of this project are;

- Analysing Ross's experimental and computational data.
- Measuring the toroidal shell's diameter at different locations initially and after each test.
- Organising an experimental procedure.
- Performing experiments.
- Analysing the experiments on computational simulation.
- Discussing and analysing the significance of the results.

The possible academic beneficiaries are listed below for this project;

- The proposed project will be beneficial for the researchers, companies and governments that are interested in toroidal shells for various applications.
- This case study will be helpful to academicians with presentations of the different configurations of toroidal shells and comparisons on them.
- By using this dissertation as a guide, academicians can understand the maximum critical pressure for different configurations of toroidal shells.
- This project might be used to for aerospace or underwater applications, for uses of toroidal shells as a pressure hull.

1.3 Outline of the Dissertation

In this dissertation proposal the literature review of the toroidal shell will be presented with different kinds of configurations and these configurations will be compared. Analytical, experimental and computational data will be presented and discussed in the literature review section. In methodology section Ross's previous experiments will be analysed. Moreover, in methodology section the procedure for measuring the toroidal shell, experiments and computational finite element analysis procedure will be presented. In results and discussions section the results will be presented and the results will try to be justified. In conclusion a brief summary of results will be presented.

2. Literature Review

This chapter covers a detailed analyse of external buckling of toroidal shells based on previous researches. The buckling of toroidal shells will be analysed in three solution ways; computational simulation, analytical and experimental. The results will be compared and failure of the toroidal shells will be presented and discussed.

2.1 Introduction

It is important to understand how buckling works on geometries. Yasir (2012) defines buckling as; “a mathematical instability, leading to a failure mode.” In theory, buckling can be caused by “bifurcation of the solution to the equations of static equilibrium” but buckling is practically defined as a “sudden failure of a structural member subjected to high compressive stress, where the actual compressive stress at the point of failure is less than the ultimate compressive stresses that the material is capable of withstanding”. For example, when a column of a bar is subjected to axial compressive load, buckling occurs if the bar deforms laterally, therefore it can be said that, buckling is instability of material elasticity. For toroidal shells under external pressures, a slight decrease on the toroid can be observed before the buckling starts into a number of circumferential waves. Blachut’s (2000) studyillustrates a visual example of buckling of a toroidal shell which is shown in figure 1. For lightweight and thin structures buckling plays an important role because the structure may fail before the strength and stiffness criteria are violated (Wang et al. 2005)

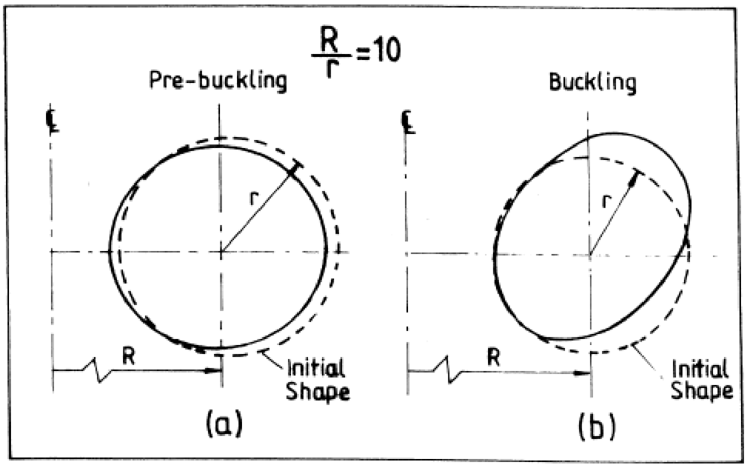

Figure 1Buckling of a Toroidal Shell

Toroid is a technical word for a doughnut or o-ring shaped object. A toroid can be generated by drawing a circle and rotating a geometric shape outside the circle.

The defects on the materials usually offer better mechanical properties for geometries. Spherical and cylindrical shells which are being subjected to external pressure are known to be highly sensitive to structural imperfections (Hutchinson, J.W. 1967) however Galletly (2000) has found on his experiments that, "circular toroidal shells are not sensitive to localized or buckling mode imperfections" moreover, about a 16% maximum decrease in buckling pressure has observed for an imperfection amplitude, w_0 , is equal to the shell thickness t, i.e. w_0/t=1 .Galletly (2000) also found out that, elliptical toroids with k-values on the ascending part behave similar to circular toroids since the elliptical toroids are not sensitive to initial imperfections of either localized or the buckling mode type.

2.2 Theoretical Buckling of a Toroidal Shells

Elasticity is a physical property which defines a structure regaining its original shape after being deformed by a force; therefore it is important to calculate the elasticity of toroids for different conditions. Wie and Bryson (1990), suggests equation 1.1 ;

$$\frac{\phi(s)}{u(s)} = \frac{1}{[J + (\pi/4)\rho R^4]s^2} \quad \textbf{(1.1)}$$

These equations were generated by Wei and Bryson (1990), considering a model which is shown in figure 2.

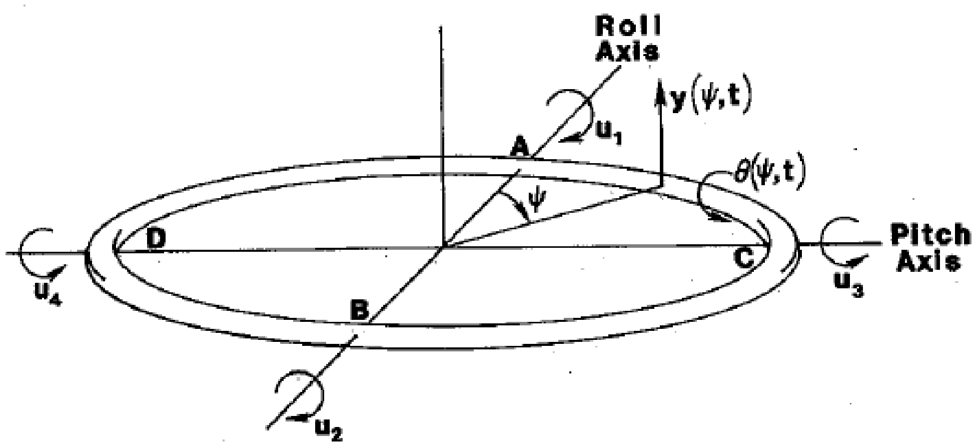

Figure 2The Elastic Buckling Model (Wei and Bryson 1990)

All the pitch axis and roll axis torque controllers are identical however; the roll axis torque controllers decoupled with pitch axis torque controllers (Wei and Bryson 1990).

A general solution was suggested by Novozhilov (1959) for symmetrical deformation of toroidal shells. Based on membrane theorem, which is generally simpler because it neglects all the moments occurs on the shell. Although this may not seem a realistic solution, for shell's which have very small bending stiffness or when the moment forces are really small to consider Novozhilov's (1959) equation can be used for a practical solution;

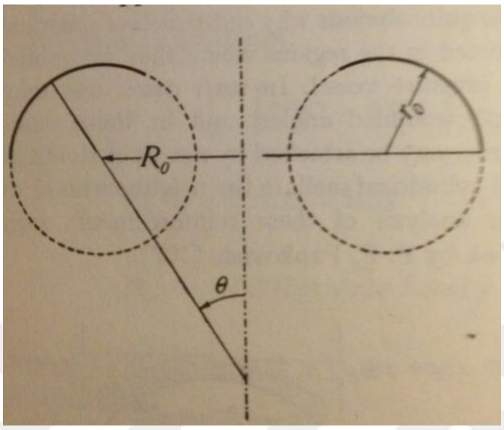

Figure 3Toroidal Shell

For the toroidal shell presented in figure 3;

$$R_1 = r_0, \qquad R_2 = R_0 \frac{1 + \alpha \sin\theta}{\sin\theta} \tag{1.7}$$

$$\propto = r_0 / R_0 \tag{1.8}$$

And for P_0 uniform static load;

$$(1 + \alpha sin\theta)\frac{d^2V}{d\theta^2} - \alpha cos\theta \frac{dV}{d\theta} + i2d^2 sin\theta V = 2d^2\tilde{D}cos\theta \tag{1.9}$$

Where;

$$D = -\left(2d^2 A + i\alpha \frac{P_0 r_0}{2}\right) \tag{1.10}$$

This equation may be the most practical equation for symmetrical loads on the toroidal shells, because the bending forces can be neglected for this example. Although it is proven that this form is successful for most of the applications, it does not has a closed-form solution (Sun 2010). Hutchinson (1967) has proven out that toroidal structures can work in higher pressures compared to cylindrical shells. The configurations of shells are given in figure 4.

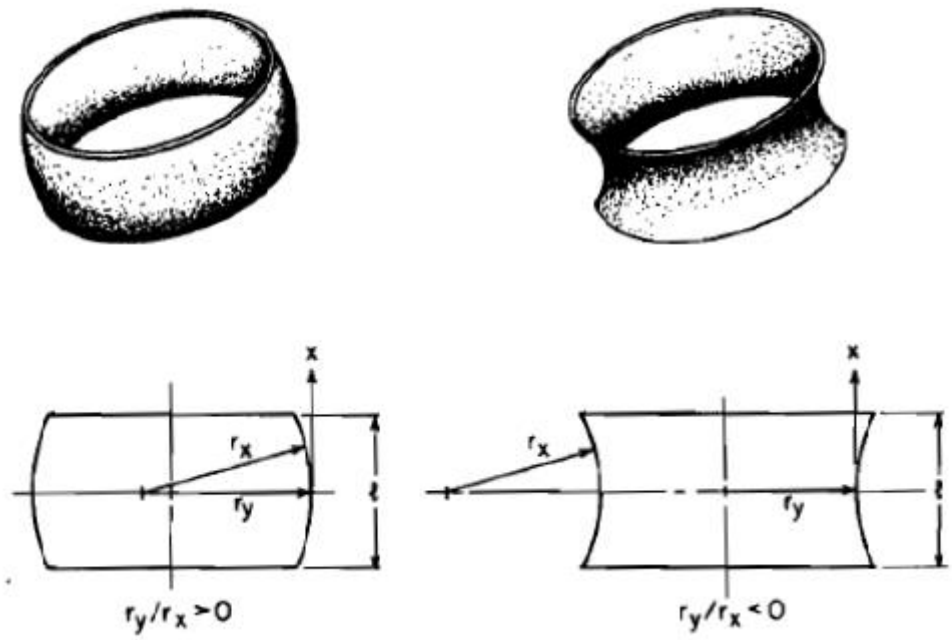

Figure 4Configuration of Shells (Hutchinson 1967)

Although Hutchinson's designs are not considered as a true toroidal shell, from his work the effect of curve can be observed for vertical loads. It can be seen bowed out shell has a significant buckling strength compared to bowed in shell. In the formula given below D is the bending stiffness where;

$$D = Eh^3/12(1 - v^2) \tag{1.11}$$

Figure 5 shows that curvature geometry is directly related with the buckling pressures, as the curve bows out the structure becomes more rigid for external pressures. It is also important to calculate the results for post buckling behaviour of the structure. For, post buckling the imperfections on the structures plays an important role. For example for a cubic load – deflection analysis has given in figure 6 below.

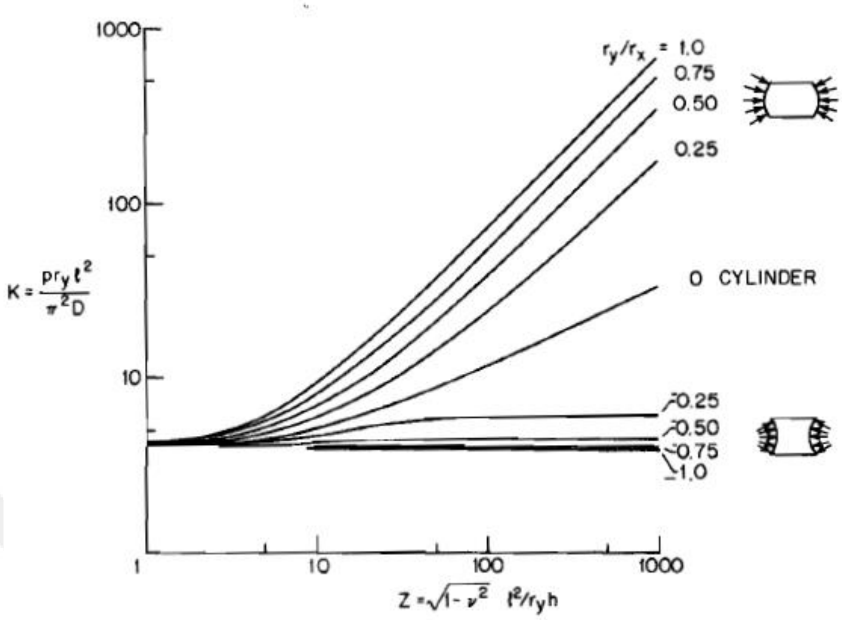

Figure 5The vertical loading of shells (Hutchinson 1967)

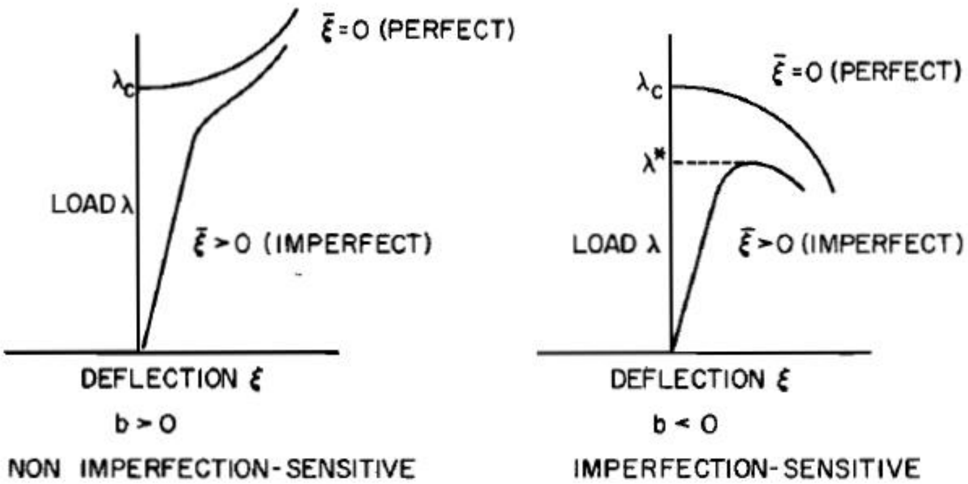

Figure 6Effect of Imperfection analysis (Hutchinson 1967)

Figure 6 represents for $\bar{\varepsilon}$= 0, is the assumption made for where the mode of deflection is 0 prior to buckling depending on the thickness of the shell. In the imperfection sensitive analysis were after the load is reduced the deflection still continues but for non-imperfection analysis load has to increase to increase the deflection has been made on the structure.

Semenyuk and Zhukova (2011) have recently made a study based on stability of toroidal shells. They have created a mathematical model of a toroidal shell by generating revolved circular arcs mathematically and defined a formula for external pressure. Semenyuk and Zhukova have found that under the external pressure the "toroidal shells can exhibit high stability where their meridional arcs are shallow." Moreover, they had found out that, toroidal shells connected with ring structures can offer a higher stability.

Plasticity is a phase which the material cannot return to its original shape after the material is subjected to a force. It is important to analyse toroidal shells as rigid plastic object to build structures which may be subjected to high forces like armour of tanks. The analytical theory of plastic buckling of a toroidal shell was developed by Skrzypek and Zyczkowski (1983) by using small strain and Naval-Davies theories for large logarithmic strains (Skrzypek 1990).

For internal plastic buckling Vu and Blachut (2009) suggests for model given in figure 7, the equation in table 2 can be used.

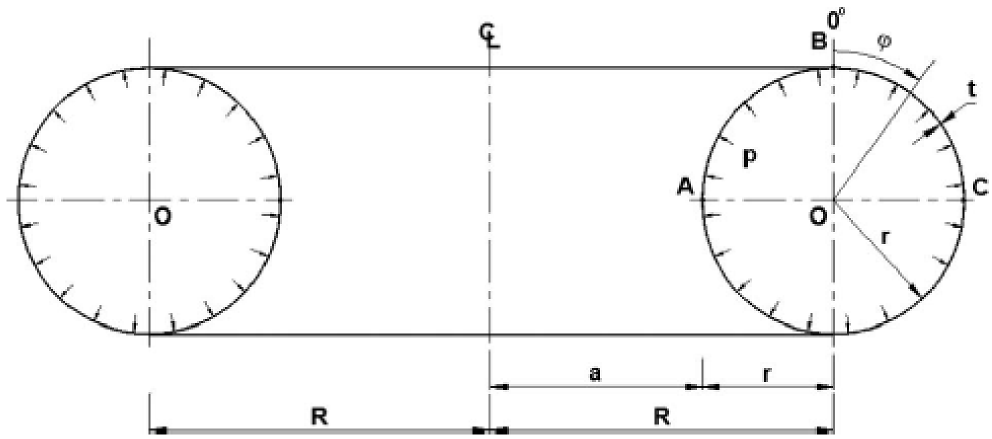

Figure 7Model for Toroidal Shell (Vu and Blachut 2009)

Table 1 Generalised stress and strain (Vu and Blachut 2009 cited in Mellor)

	Uni-Axial Tension	Internal Pressure of Toroidal Shell
$\bar{\boldsymbol{\varepsilon}}$	$n - B$	$\frac{2n}{3}\left(\frac{1}{(1-x+x^2)^{1/2}} + \frac{(x-2)(x-1)}{2(x^2-x+1)^{3/2} - (2R/r-1)}\right)^{-1} - B$ where; $x = \left(\frac{R/r-1}{2R/r-1}\right)$
$\frac{\bar{\boldsymbol{\sigma}}}{\boldsymbol{A}}$	n^n	$\left(\frac{2n}{3}\left(\frac{1}{(1-x+x^2)^{1/2}} + \frac{(x-2)(x-1)}{2(x^2-x+1)^{3/2} - (2R/r-1)}\right)^{-1}\right)^n$ where; $x = \left(\frac{R/r-1}{2R/r-1}\right)$

The value of A is a measure of hardening and n is the increment rate of the hardening. B defines a "measure of initial state of the material". For plastic instability pressure Vu and Blachut suggests the following formula (2009) for vessel;

$$\begin{aligned}(nz - B)r = &-2\sqrt{3a^2 + 3ar + r^2} \\ &- \sqrt{3}r \ln\left(\frac{\sqrt{3}r}{2} + \sqrt{3}a + \sqrt{3a^2 + 3ar + r^2}\right) \\ &+ 2r\ln\left(\frac{2r^2 + 3ar + 2r\sqrt{3a^2 + 3ar + r^2}}{a}\right) + 2\sqrt{3a_0^2 + 3a_0 r + r^2} \\ &+ \sqrt{3}r\ln\left(\frac{\sqrt{3}r}{2} + \sqrt{3}a_0 + \sqrt{3a_0^2 + 3a_0 r + r^2}\right) \\ &- 2r\ln\left(\frac{2r^2 + 3a_0 r + 2r\sqrt{3a_0^2 + 3a_0 r + r^2}}{a_0}\right)\end{aligned} \quad \textbf{(1.12)}$$

where;

$$\bar{\varepsilon} = (nz - B)r \quad \textbf{(1.13)}$$

This equation when compared to experimental data the following chart has obtained by Vu and Blachut (2009);

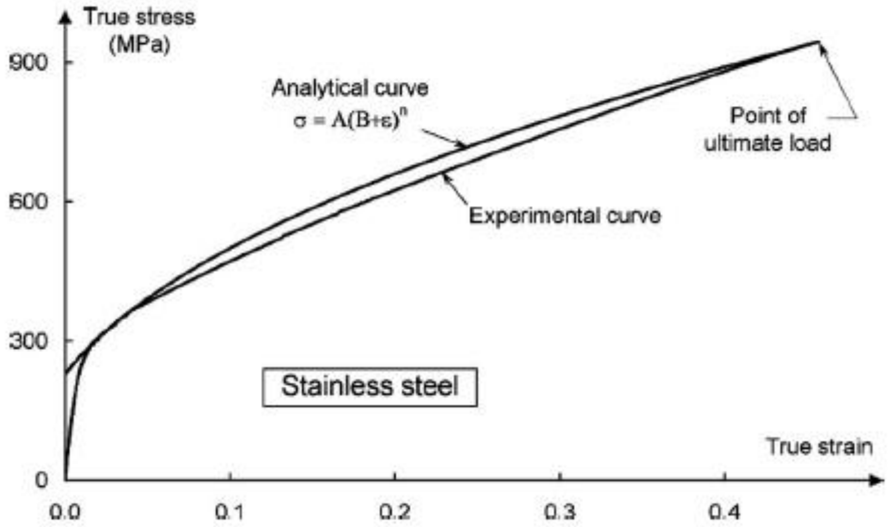

Figure 8Comparison with analytical data and experimental data (Vu and Blachut 2009)

The toroidal shells were produced by welding four elbow parts from stainless steel. The toroidal shells were filled with oil by manually pumping the oil inside the shell. Comparing analytical values with experimental values, the analytical values found to be always less than the experimental values. The error range has found to be between the range of -9.6% to 7.5% (Vu and Blachut 2009).

2.3 Previous Experimental Researches

The most recent study on toroidal shells has been made in the University of Liverpool by Michael Ross (2013). Ross has conducted an experiment by using Denison compression test machine, which is capable of using 3000 kN force. The toroidal shell which was used on the experiment is given in figure 9.

Figure 9Experimental toroidal shell

As can be seen from figure 9, four elbow parts have been produced by rolling and extruding. The toroidal shell has been produced by welding. The thicknesses of the parts pointed with dots have been measured. The mechanical properties are not homogenous since there are four welded lines, therefore this may have affected Ross's experiment. The testing apparatus is shown below in figure 10. The test equipment was controlled manually and the test has been done time independent. In the test it is observed that right after the loading has done the toroidal structure shows spring-back effect, therefore it may be important to calculate the spring back effect on the toroidal shell for external pressures. Moreover, for single elbow parts the spring back effect is observed to be more effective.

The cylindrical apparatus at the top and bottom of the toroidal shell are not clamped to the compression machine that is why; the top apparatus is causing an extra force on the toroidal shell.
The results of Ross (2013) are given on the figure 11 below for 2 mm. thick toroidal shell for horizontal loadings.

Figure 10Testing Apparatus

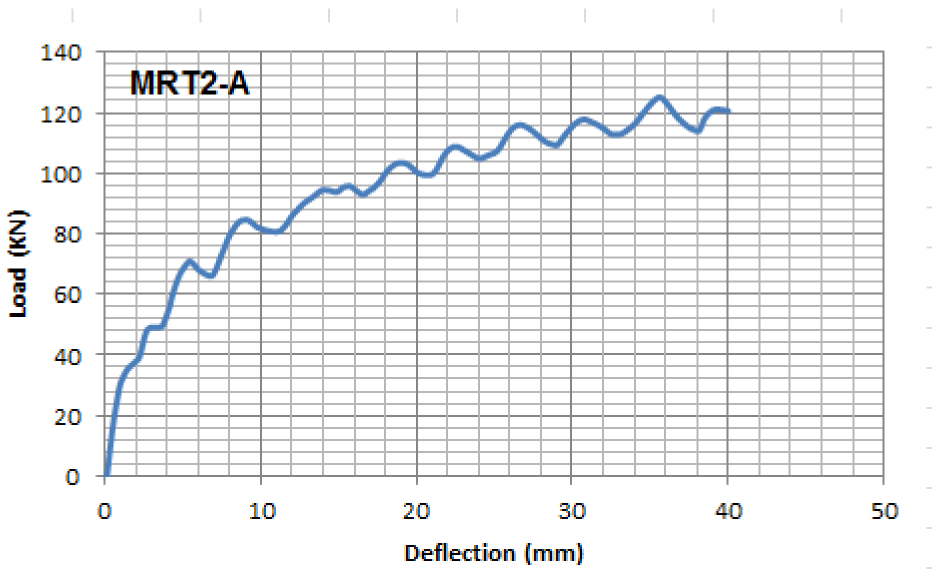

Figure 11Experimental Results (Ross 2013)

The fluctuations and the graph may be explained by the spring back theory. Spring back can is elastic recovery of a material. It is caused by the residual stresses. It can be seen that the material has shown a solid deflection till the load is 38 kN. The elastic limit of the structure can be defined as 38 kN. The deflection calculated by the mean value of four different points' deflection. Compared with a 3 mm. thick toroidal shell, 2 mm. thick shell shows less rigid structure. The 3 mm. thick shell graph is given in figure 12.

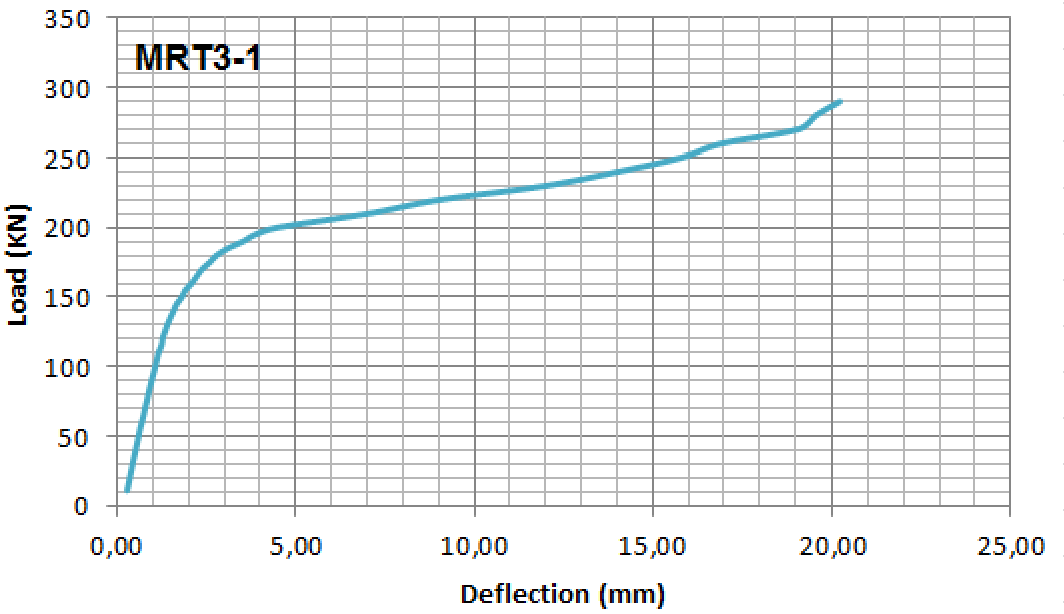

Figure 123 mm. shell deformation vs. load

Figure 12 shows less fluctuations and a more rigid structure. The elasticity point is around 150 kN, which is almost five times higher than the 2 mm. thick toroidal shell. Ross's (2013) experiments show that between 3 mm. thick toroidal shell can operate at five times higher external pressures compared to 2 mm. ones. To analyse the importance of thickness more researches are needed to be done.

2.4 Previous Computational Simulation

Computational simulation analyses may give the most accurate result, since they are able to work in high mesh densities. For buckling, analysis generally BOSOR and ABAQUS software programmes are being used to analyse the deformation on the parts. Blachut (2004) has a study on uniform external pressures, made by woven fabric. The material properties which were used in the analysis is given in table 1.

Table 2 Material Properties (Blachut 2004)

Material	E_{11} (GPa)	E_{22} (GPa)	G_{12} (GPa)	ν_{12}
Woven	70.0	70.0	5.0	0.1
Unidirectional	140.0	10.0	5.0	0.3

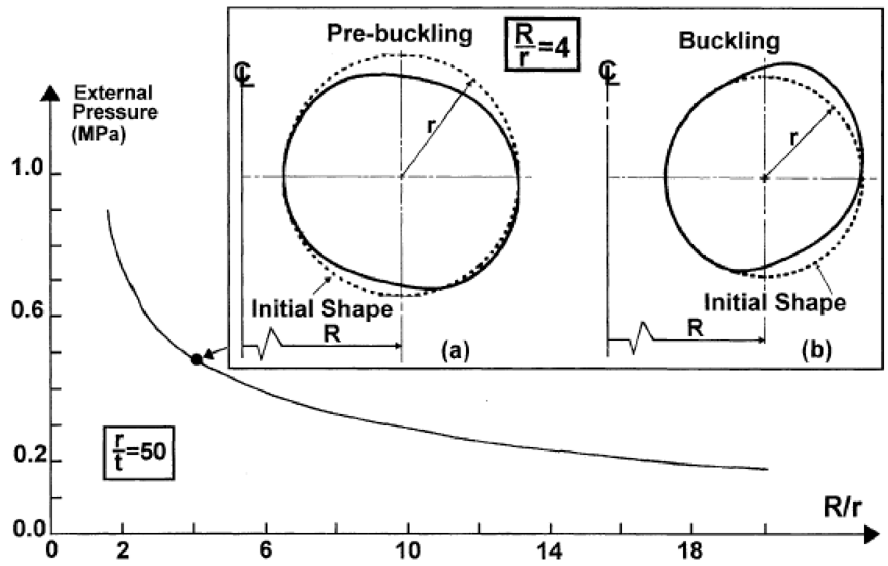

Figure 13Bifurcation pressures of woven (Blachut 2004)

For smaller R/r the toroid can maintain more solid structure. This analysis is important for toroidal structures, which will be subjected to uniform external pressures. It can be seen that the woven structure absorb close to 1.0 MPa. Blachut (2004) has carried on the research by changing the material properties to Aluminium. Figure 13shows the results for toroids which are made by different materials.

As can be seen from figure 14, aluminium configuration can sustain up to 9 MPa. Figure 15 shows the pressure distribution on the North Sea with Blachut's aluminium hull configuration a submarine can operate up to 1 km depth; moreover with a stiffer configuration with composite materials a higher-resistance hull can be produced.

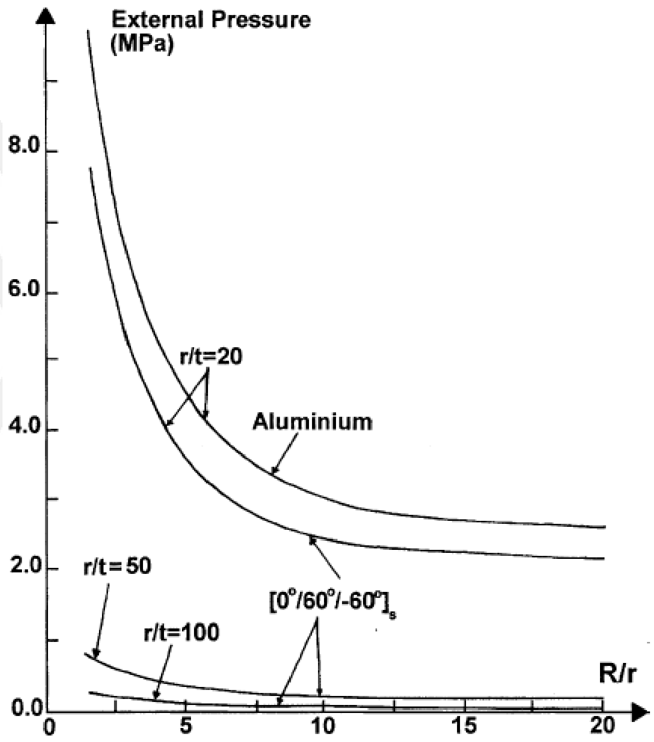

Figure 14Buckling pressures for toroids (Blachut 2004)

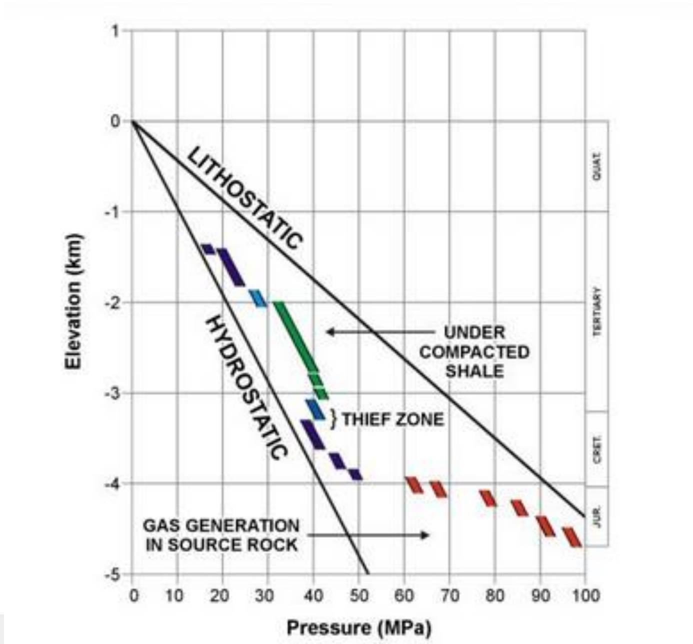

Figure 15Pressure Profile North Sea (Crain ND)

Prolate and oblate elliptical cross-sectional toroids shells have also considered at Blachut's study (2004) since they can show a higher resistance. Figure 16 shows the buckling pressures versus semi-axis ratios.

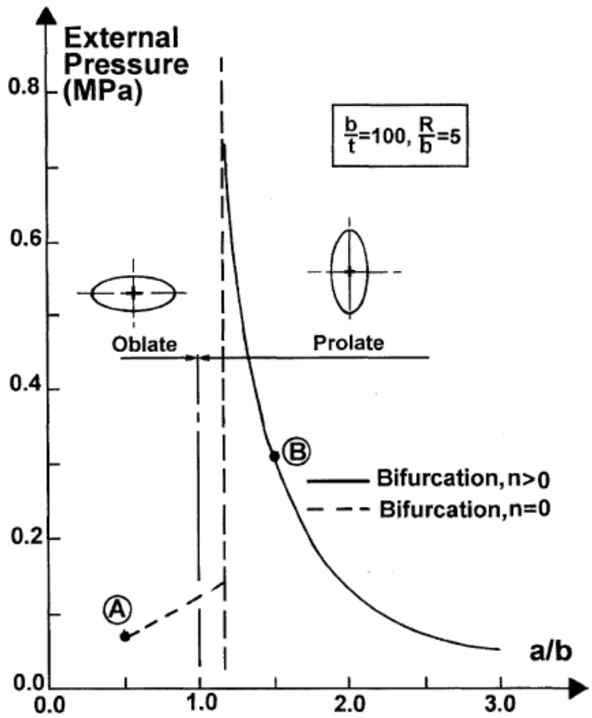

Figure 16 Elliptical Shells' Birfurcation Buckling Pressures (Blachut 2004)

From figure 16 it can be seen that there is a sudden change for at a/b=1.17. Figure 16 also shows that elliptical toroidal shells can absorb higher damage (Blachut 2004), therefore in the use for pressure hull applications elliptical toroidal shells can be a better choice. Also the buckling pressures for different rotational cross sections have been given in figure 17.

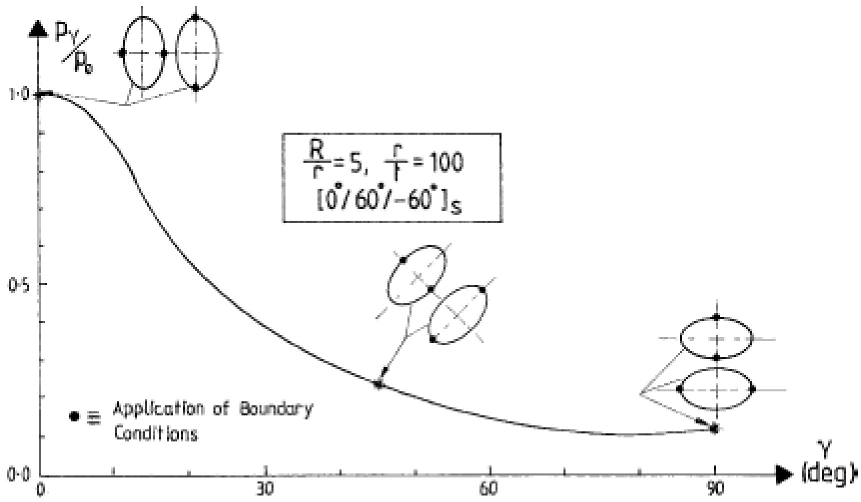

Figure 17Rotation vs. Buckling Pressure

Elliptical cross-sectional toroidal shell studies are also made by Galletly (2000). His model is given in figure 18 below. He discovered that toroidal shells for elliptical cross-sections have stiffer structure. For k=a/b vs. critical pressure graph is given in figure 19 for two different toroidal shell configuration. It can be seen that ask value approaches approximately 1.85 the configuration becomes more stable. When compared to toroidal shells with circular cross sectional areas which is, k=1 , while k=1.85 Galletly's (2000) toroidal shell configurations' critical pressures are almost double for a non-imperfect configuration.

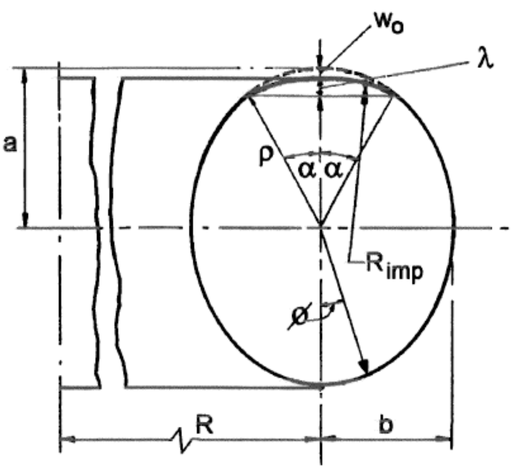

Figure 18Galletly's model

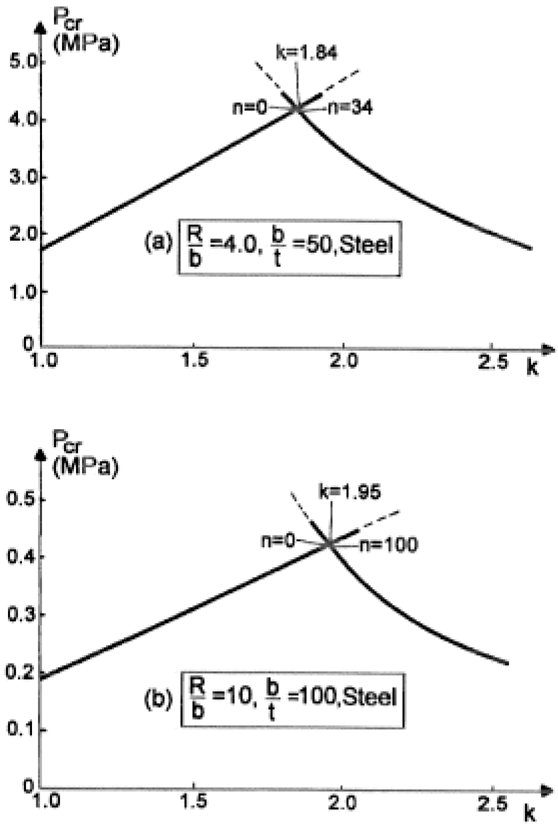

Figure 19k vs. Pcr (Galletly 2000)

Although figure 19 shows a stable configuration of a toroidal shell would have around k=1.85, when imperfections are taken in to account the solution changes. In figure 20 it can be seen that around k=2.15 the toroidal shell becomes more stable. From the figure 20 it can be seen that, imperfections may play a big part since for k=1.85 critical buckling pressure is around 2.0 MPa while for k=2.16 critical buckling pressure is around 2.6 MPa.

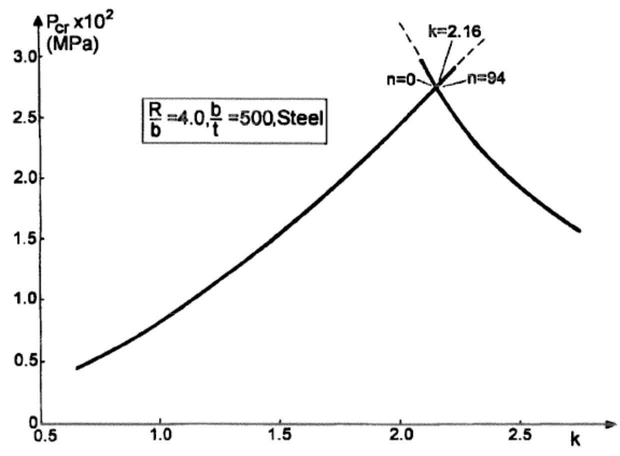

Figure 20Toroidal shell k vs. Pcr with imperfections (Galletly 2000)

Wang and Redekop(2006) have made a research based on vibration and buckling of toroidal shells using ADINA commercial finite element software analysis. In the analysis they used four stiffeners to observe the effect of stiffeners on the toroidal shells on buckling and vibration conditions. The model used for the computational analysis is given in figure 21.

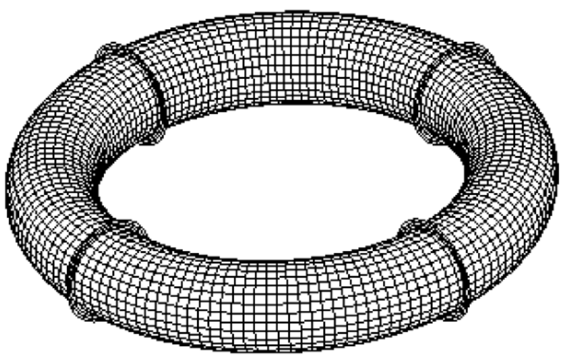

Figure 21The toroidal model with four stiffeners (Wang and Redekop 2006)

Wang and Redekop has found in their researches that, four ringed structure is more rigid compared to simple toroidal shell without any ring, however when compared to heavy ring structure, to light ring structure, light ring structure can resist a higher buckling pressures. Although the structure can resist to higher buckling pressures, as the ring number increases the vibration frequency increases (Ibid). The results also show that, inner and outer equatorial supports show a higher support for buckling pressures (Ibid). In figure 22 a design for nuclear reactors is given below,

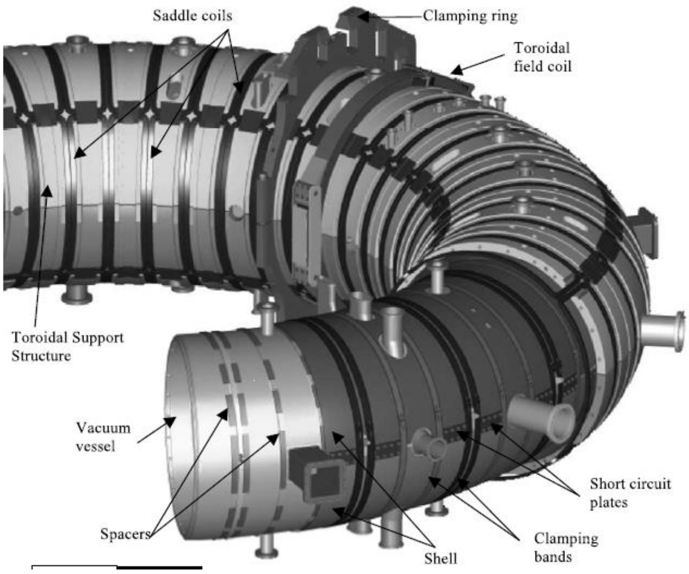

Figure 22Toroidal Shell for RFX designs (Baker et al. 2002)

In the example the toroidal shell is subjected to internal pressure. Toroidal shells are also being used to transport high pressurized fluids. This example in figure 22 is a usage of toroidal shells subjected to internal pressures. This mechanism can safely operate in the conditions given in figure 23.

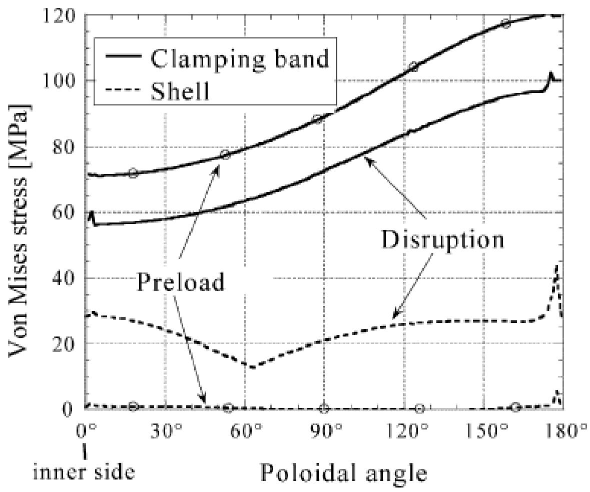

Figure 23Operating Conditions (Baker et al. 2002)

Wang and Redekop's design with stiffener rings might increase the inner pressure in the toroidal shell, which may be compensate higher external buckling pressure. For space or underwater missions it may be considered to increase the internal pressure by injecting high pressurized gas or liquid to maintain the toroidal shells stability at higher pressures. For example, for submarines to maintain high pressures toroidal shell designed for nuclear reactor can be used to store exhaust gases. By using this technique the toroidal shells may operate at higher external pressures, to balance the internal pressure caused by a safety valve mechanism can be used.

At figure 24 Ross's (2013) computer analysis results have given for horizontal loading. It can be seen that thicker toroidal shell is a more rigid structure, which is also proved by Ross's experimental study. The elastic limit of the structures for 1.9 mm. shell it is around 8 kN and for 2.2 mm. thick shell it is around 15 kN,which this is nearly double of the thin shell.These results show that buckling of a toroidal shell is highly depended on the thickness of the shell. Moreover, a stiffer structure may be obtained by increasing the thickness and changing the cross-sectional geometry to an ellipse.

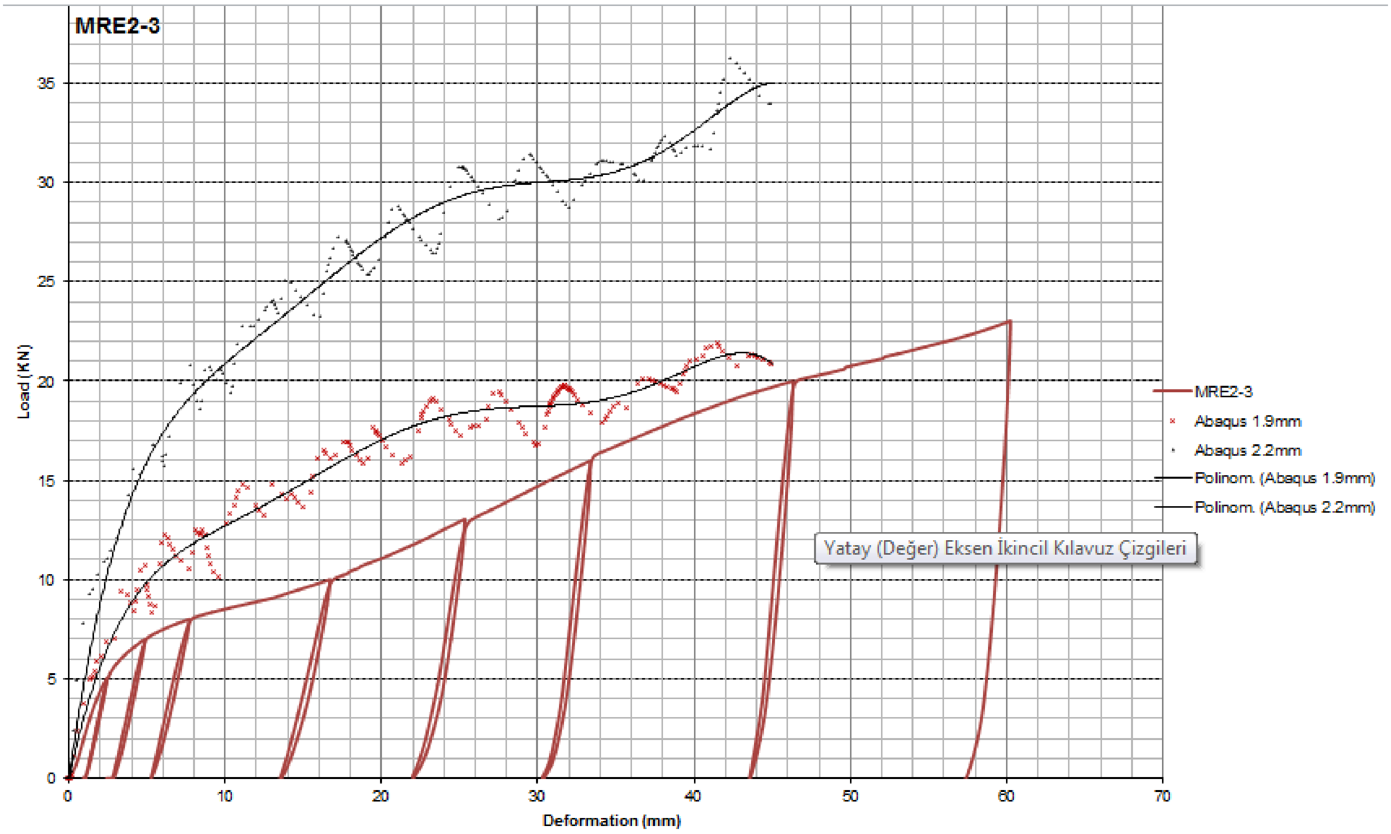

Figure 24Abaqus Analysis (Ross 2013)

Zhan and Redekop (2007) have made a research based on the usage of toroidal shells as a liquid petroleum gas (LPG) tank. After the petroleum prices went higher, LPG has become a better alternative fuel source in some countries; however after the first LPG tanks introduced there had been many accidents due to explosion of the tank. After studying structural analysis of materials toroidal shells were found to be a good alternative to cylindrical shell. Their study has found out that, wall thickness has the greatest influence on the buckling pressure.

The toroidal shells are also being used as a pressure vessel. In those cases it is important to calculate the internal pressures caused by the fluent. Although analytical solutions are important to find an optimised design, with computers a more detailed analysis can be done. Galletly's (1998) toroidal model is shown in figure 25.

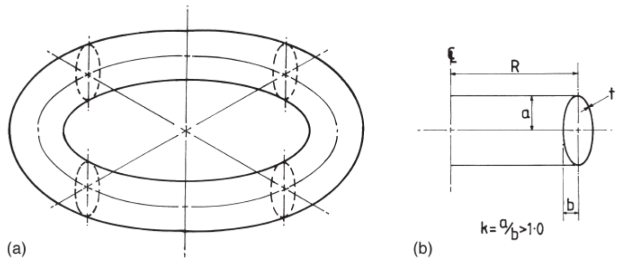

Figure 25Galletly's toroidal shell model (Galletly 1998)

He has found that as the ratio of a/b increases the stability of the toroidal shell decreases for internal pressures. Moreover, he has found that as the ratio of R/b decreases the stiffness of the toroidal shell increases for internal pressures. The diagram for the relationship between a/b and R/b is given in figure 26.

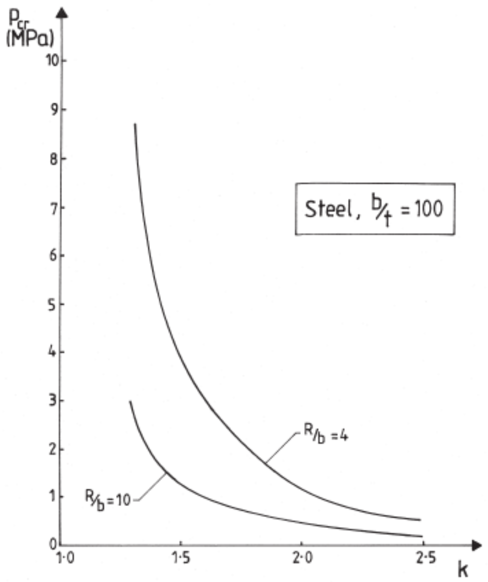

Figure 26R/b vs. a/b (Galletly 1998)

Another alternative for pressure vessel is cylindrical tanks. Cylindrical tanks are widely being used mainly for heating of the residences. While these tanks are used as a pressure vessel, having an equal pressure distribution can offer higher advantages like the material can stay stable in higher pressures or the mechanical endurance of the structure can be increased. The pressure distribution for a cylindrical shell is given in figure 27.

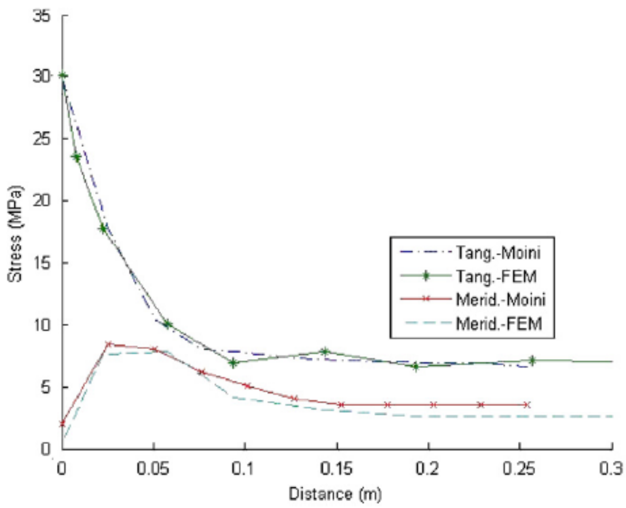

Figure 27Tangential and meridional stresses inside a cylindrical shell for internal pressures (Zhan and Redekop 2009)

From the figure it can be clearly seen that the distribution of the pressure changes almost three times along the tangential line of the shell. For toroidal shells the pressure distribution varies with the ratio of radiuses. For Vu and Blachut (2009)'s model shown in figure 7, the distribution of the pressure is given in figure 28.

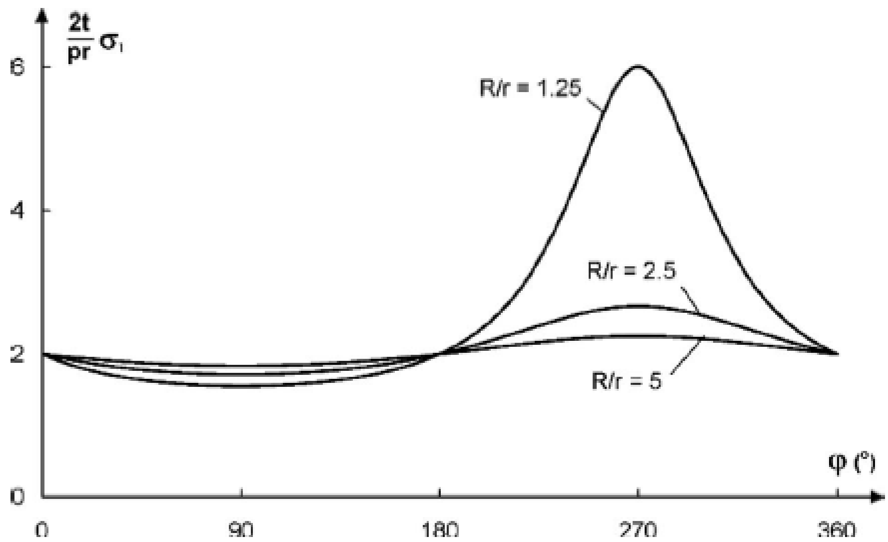

Figure 28Pressure distribution of a toroidal shell

From the figure it can be seen that as R/r ratio increases the pressure distribution can be maintained more homogenously. Moreover, as R/r ratio decreases the pressure is more likely to be higher at 270 φ region. In some cases, it is desired not to have an equal pressure distribution. For example, for a R/r=1.25 toroidal shell it is more easier to find the failing part in case of a failure compared with a R/r=5 toroidal shell.

2.5 Conclusion

Different kinds of designs and analysis have been presented and discussed in literature review section both for external and internal loadings. It is seen that elliptical toroidal shells can maintain its stability at higher pressures. The imperfections play an important role at buckling of toroidal shells and for structures which needs to work around critical loadings, a detailed imperfection analysis may be needed. From the theoretical point of view, Vu and Blachut's study give a realistic result when compared to experimental values. In the future, the buckling of internally pressured toroidal shells, subjected to external pressures can be studied for submarine applications, since it can offer to maintain working at higher values of pressure.

3. Methodology

Methodology is an algorithm offers an acceptable solution for a problem stated in the introduction of the project, by using analysis, design, simulation and experimentation techniques (Burback 1998). The purpose of this chapter is to provide information for the reader to explain which methods have been used to gather data to find the solution for the problem. This section presents the structure of the research and the assumption that have been made to obtain solution.

Qualitative research technique has been used to gather data for this project. According to Arghode (2012) the researcher seeks to find the solution based on the experiments and utilizing scientific methods primarily. In this project two experiments have been conducted by the supervision of the University of Liverpool personnel and supervisor of the project. The experiments have been validated by using ABAQUS software, computer integrated finite element analysis.

The methodology section has been divided into two parts one is experimental part and the computational simulation part. In experiment part the experiment procedures and measurement techniques will be explained. In computational model part the model and the assumptions will be presented.

3.1. Experiments

The experiment section has been conducted in three parts;

- Analysing the experimental values of Ross's test (2013);
- Measuring the toroidal shell specimen;
- Testing the specimen;

3.1.1. Analysing Ross's Test

By welding four 3" 90° elbows the toroidal shells were constructed (Ross 2013). The mig welding has been done through a V-prep by WREN Industries to minimise the gaps (Ibid). The toroid model drawing has been shown on figure 29. By extruding the steel 316/316L material the elbows were constructed (Ibid). The wall thickness and the radius of the toroidal shell vary on different regions. This may be the cause of how the manufacturing was done by the manufacturer.

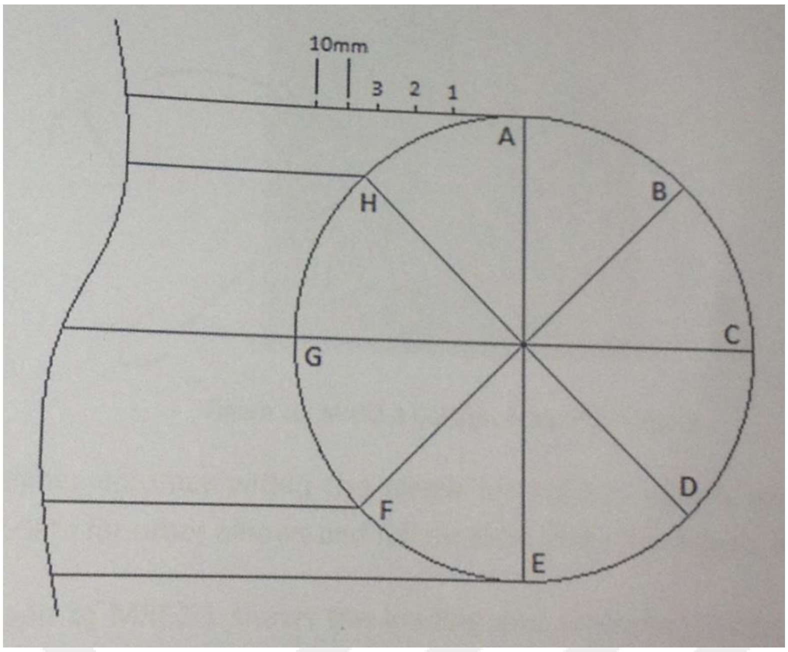

Figure 29Toroidal shell drawing (Ross 2013)

Figure 1 shows the lines which were drawn on the toroidal shell. Every line was divided into 80 pieces to determine the points to make measurements. The thicknesses of the elbows were measured using Teledictator 2000 and the radiuses were measured using a digital calliper with both ± 0.005 mm. accuracy. The measurement data was shown on table XX.

Table 3 Toroidal Shell Measurements (Ross 2013)

	Toroidal Shell
D (mm.)	228.56
d (mm.)	85.74
t (mm.)	2.06

Ross has conducted the first stage of the experiment using Instron 4505 compression machine with 100 kN load cell (Ross 2013). The force applied by Instron is controlled by servo motor system and it is measured by strain gauges (Ibid). Three flat plates were used, one is above and the other two are below at the specimen to apply load homogenously and not to damage the Instron machine. The increase and decrease on the load rate can also be controlled by the machine.

The experiment has started with a load rate of 0.1 mm/min and it increased up to 2mm. (Ross 2013). After 2 mm. deflection on the toroidal shell the loading rate has increased to 0.25 mm/min. until it reached to 98.7 kN. The load did not increase to 100 kN because of safety reasons. The design procedure followed the following steps (Ross 2013);

- The jaws of the Instron has opened to enable to insert plates,

- Plates and toroidal shell were inserted.
- The jaws were closed and the plates were tied.
- The parameters were set for program.
- The machine has opened.
- The measurement devices were calibrated.
- The test has started.
- The load rate was monitored and changed where necessary.
- When the desired load has reached, the machine load rate increase has been stopped.
- The unloading at a rate has been started after reaching maximum load.
- After the load on the specimen has reached back to 0 kN,
- The machine has stopped.
- The specimen and the plates were recovered.
- The test data has been obtained.

Although on Instron machine the users can monitor the deflection dial test indicators could be used to monitor the changes on different areas of the test object. Figure 30 below shows the configuration of experiment which Ross has conducted.

Figure 30Instron test configuration (Ross 2013)

The results Ross has found is given on figure31.

Figure 31 Deflection vs. Load First Test (Ross 2013)

3.1.2. Measurements of Toroidal Shell

To justify the results of Ross catalogue values for 3” elbows and measurements on 3” elbows have been conducted. The internet catalogue values were taken from Caylor Industrial Sales Inc.’s website. The measurements were made by using Mitutoyo 300 mm. digital calliper at metal workshop at the University of Liverpool. In total 80 measurements were made and the table for measurements can be seen on appendix xx. The mean values for elbow measurement is given at table xx using Ross’s model shown on figure 29.

Table 4 Initial measurement data

Toroidal Shell	Ross’s values (mm.)	Elbow measurements (mm.)	Catalogue Values (mm.)
A-E	-	88.69 ± 0.45	-
B-F	-	89.06 ± 0.24	-
C-G	-	89.12 ± 0.31	-
D-H	-	88.66 ± 0.34	-
Average diameter (mm.)	85.74	88.88 ± 0.40	88.90

Ross has not indicated if the diameter measured was inner diameter or outer diameter of the toroidal shell but adding the thickness gives a closer value to catalogue value.

The measurement data could not be found, that is why the project continues with the elbow

$$85.74 + (2 * 2.06) = 89.86 \tag{3.1}$$

measurements. The outer diameter measurements were made by using Mitutoyo 640 mm. digital calliper at the University of Liverpool metal workshop. The standard deviation and mean values have been calculated using Excel's average and stdev.s functions. STDEV.S function uses the following equation to find the standard deviation (Microsoft 2013).

$$\sqrt{\frac{\sum(x-\bar{x})^2}{(n-1)}} \tag{3.2}$$

3.1.3. Testing the Specimen

Dartec Universal Compression machine has been used to make further experiments on the specimen, at University of Liverpool Engineering School. Dartec is capable to apply 250kN maximum load and the applied force can be measured by strain gauges. The displacement can be measured with displacement transducer. The power is supplied by high pressurized hydraulic power which is supplied by the pumps.

In total four tests have been done and the chart for tests can be seen on appendix xx. The experiments were started with 0.1 mm/min load rate, at 90 kN the load rate has been increased 0.2 mm/min. The test followed following actions;

- Inserting the plates and toroidal shell.
- By using a ruler sliding the plates in the middle of the specimen.
- Placing the dial gauges and setting them to 0.
- Starting the machine.
- Starting the programme.
- Entering system parameters.
- Monitoring the force, displacement and dial gauges.
- When the desired load has been reached, unload at a rate.
- After the load reaches 0 kN stop the machine recover the specimen.

After every test measurements have been made using the same procedure explained in measurements of the toroidal shell section.

Figure 32 Toroidal Shell Test

3.2.1. Abaqus Analysis

A quarter toroidal shell model has been created to analyse toroidal shell's behaviour. The part was cut in partitions to obtain a higher quality mesh. The assembly of the model is shown in figure 33.

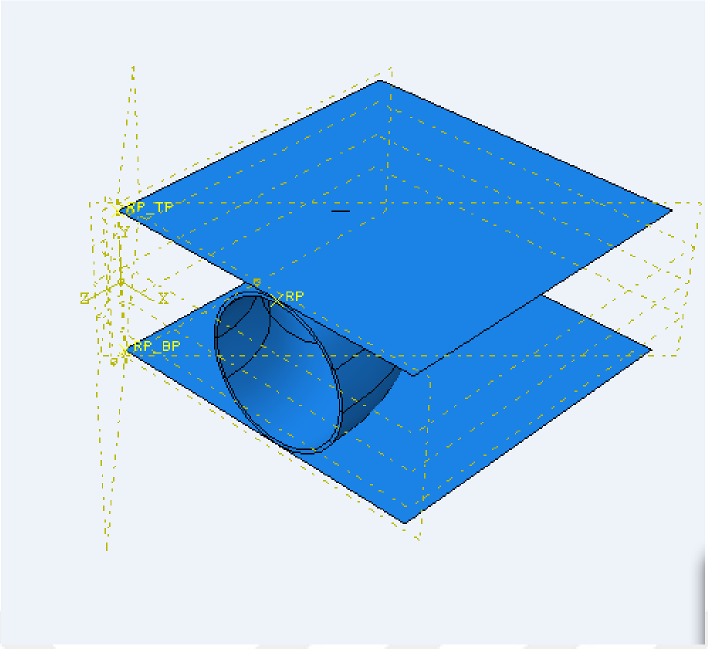

Figure 33 Quarter Model Assembly

Two symmetry planes were defined to obtain a full toroidal shell. The reason the quarter toroidal shell was created is to reduce the total solution time and increase the finer mesh size to obtain more accurate result. 3-D brick elements were used on the toroidal shell part and two 3D discrete plates were created. Material properties are gathered from Ross (2013 cited in Truong &Blachut) as shown at table XX;

Table 5

Young's modulus E (GPa)	186
Poisson's ratio	0.238
Yield Stress (MPa) (based on 0.2% strain)	245
Ultimate Stress (MPa)	598
Strain at Ultimate	0.433

The bottom plate has been assigned as encastre constraint and the top plate's movement on all directions other than vertical direction has been restricted. Figure 34 shows the input load for the toroidal shell.

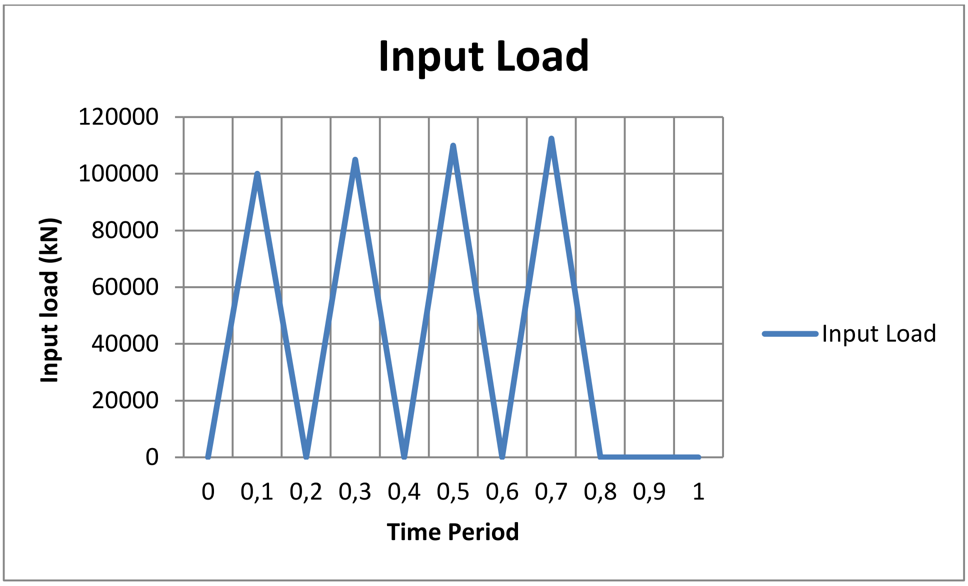

Figure 34 Input Load

Between every input leaving some time period on 0 load might be had been more realistic but this would cause more time for ABAQUS to solve the problem because in that case the time step needs to be decreased. The interaction between two plates is defined as hard contact and there is a penalty defined for friction on both plates which is 0.1. C3D8R structured meshes were created to obtain more accurate result as can be seen in figure 35 and figure 36.

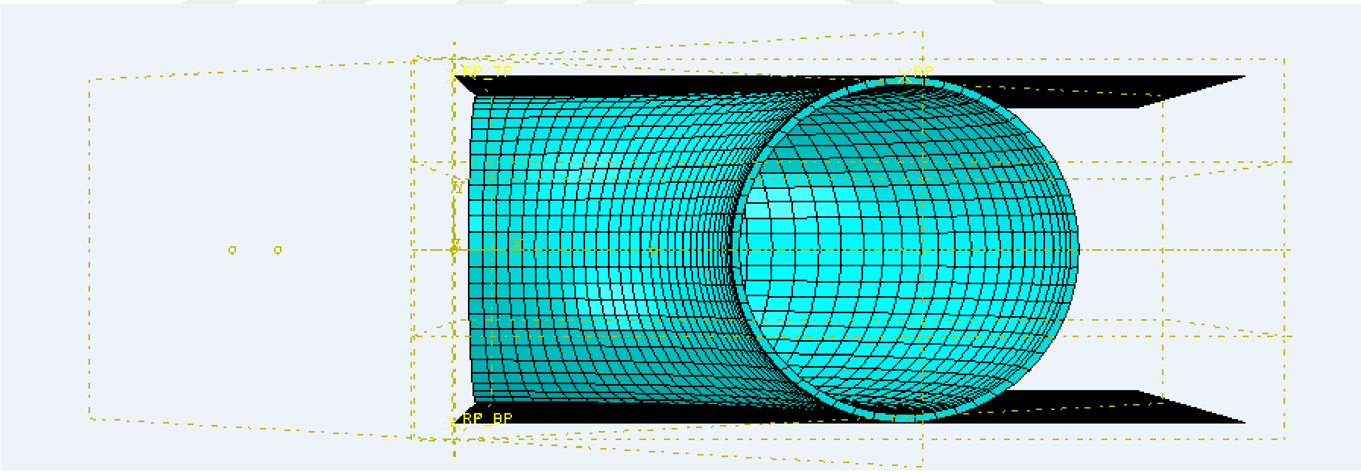

Figure 35 Meshed Front View

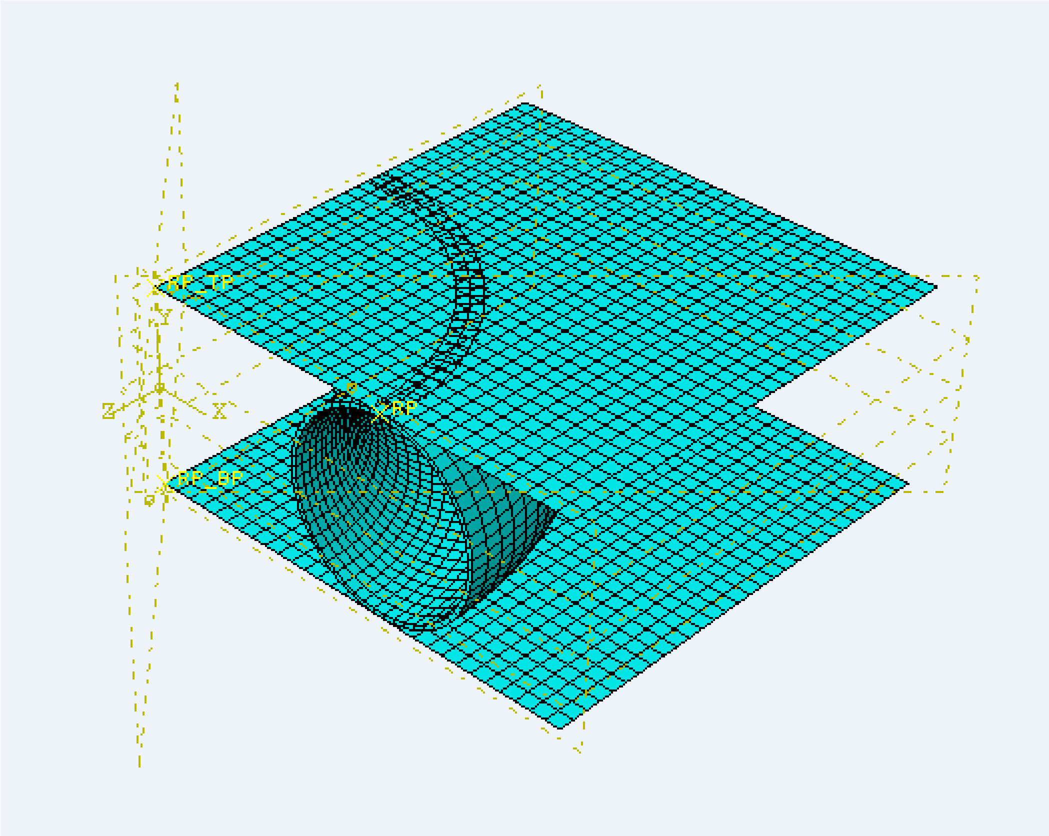

Figure 36 Isotropic Meshed View

4. Results and Discussion

4. 1.Test Results

In total three tests have been demonstrated. The results of the test data is given at appendix xx. The first test’s result has been given at figure 37.

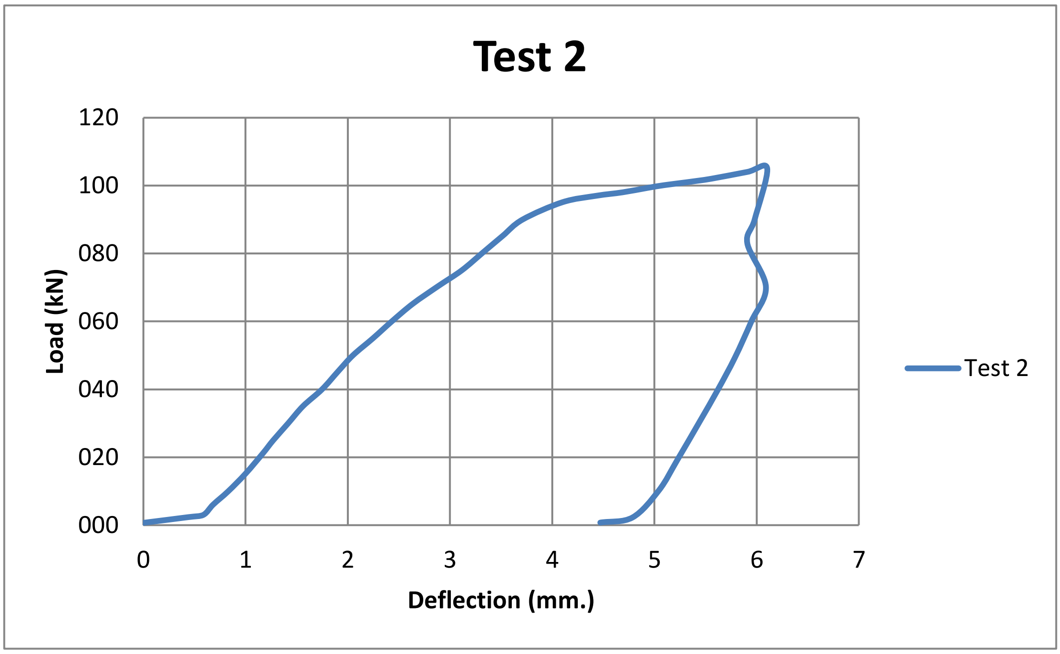

Figure 37 Test 2 Deflection-Load

Comparing with figure 31 the deflection load curve while the toroidal shell is loading is similar to test 1’s unloading curve as can be seen at figure 37. However, test 2, after it reaches to 40 kN it does not follow the same trend and follows a more similar path to loading curve.

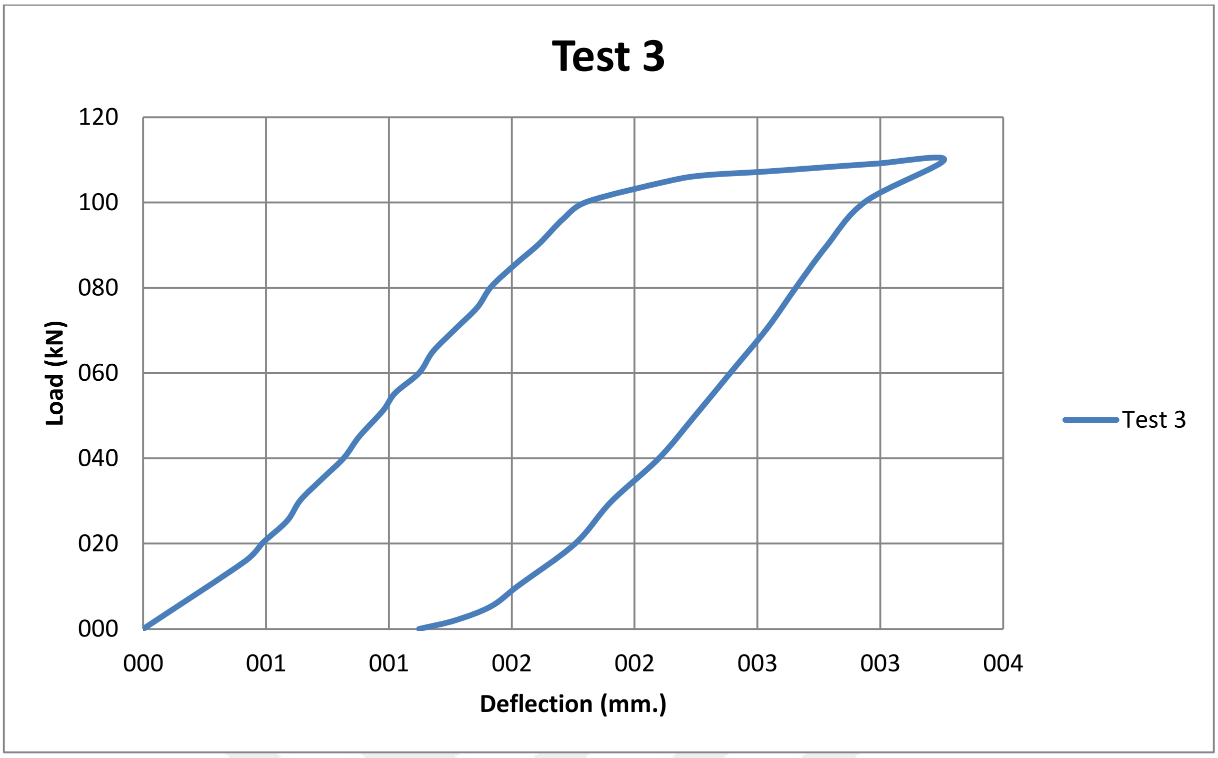

Figure 38 Test 3 Load-Deflection

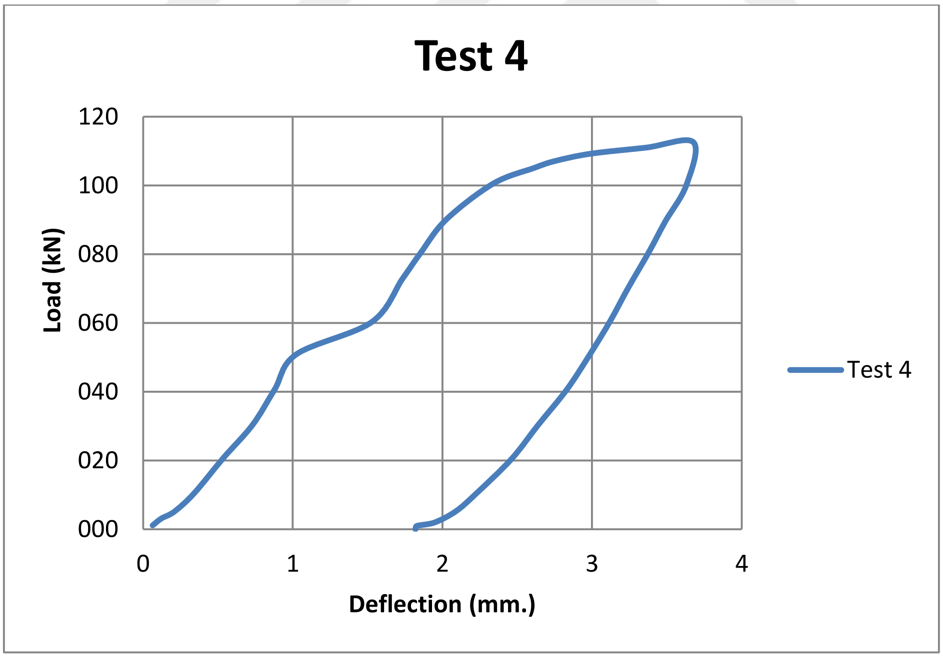

Figure 39 Test 4 Load-Deflection

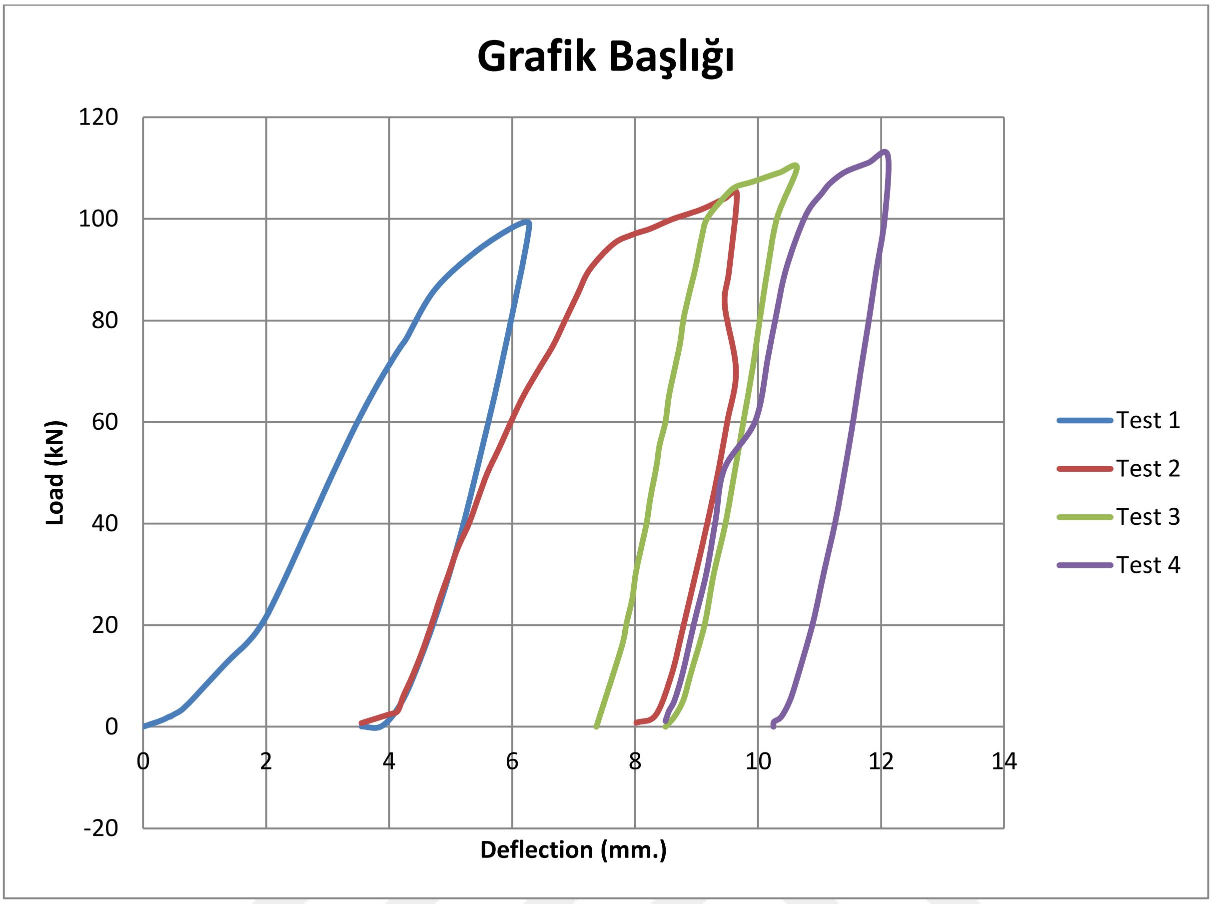

Figure 40 Combined Test

It can be seen that compression test increases the stiffness of the toroidal shell. The load-deflection curve decreases in further tests and the toroid becomes stiffer as it does not deform the same rate on the same load rate. This can be explained by density increase. The relationship between density and stiffness can be explained by the equations shown below;

$$F = k * x \tag{4.1}$$

$$F = m * a \tag{4.2}$$

$$m = V * d \tag{4.3}$$

$$k * x = V * d * a \tag{4.4}$$

Table 5 shows the measurement results after each test. As can be seen from table 5 while C-G regions diameter decreases dramatically, the A-E regions diameter does not increase the same rate and this may cause a density increase on the material and this may the primary reason on stiffness increase of the toroidal shell. This is also causing the toroidal shell to become more ductile. Also an increase on standard deviation can be observed. This is because the radius on welding points increases more than the radius on the toroidal shell side as can be seen on figure 41. Moreover, because the model was created by welding the deformation did not happen homogenously.

Table 6 Measurement Values

Toroidal Shell	Elbowmeasurements (mm.)	First Test Measurements (mm.)	Second Test Measurements (mm.)	Third Test Measurements (mm.)	Forth Test Measurements (mm.)
C-G	88.69 ± 0.45	89.67± 1.23	89.46± 1.47	89.24± 1.54	89.42± 1.70
B-F	89.06 ± 0.24	89.20 ± 0.77	89.30 ± 0.40	89.45 ± 0.57	89.87 ± 0.95
A-E	89.12 ± 0.31	85.57 ± 0.31	83.40 ± 1.01	82.32 ± 1.48	81.33 ± 1.83
D-H	88.66 ± 0.34	89.38± 0.62	89.18± 0.66	89.40± 0.75	89.72 ± 0.67
Averagediameter (mm.)	88.88 ± 0.40	88.45 ± 1.86	87.83 ± 2.77	87.60 ± 3.30	87.58 ± 3.90
Outer diameter	317.44	319.57 ± 2.45	320.21 ± 3.39	320.12 ± 3.07	320.6 ± 3.65

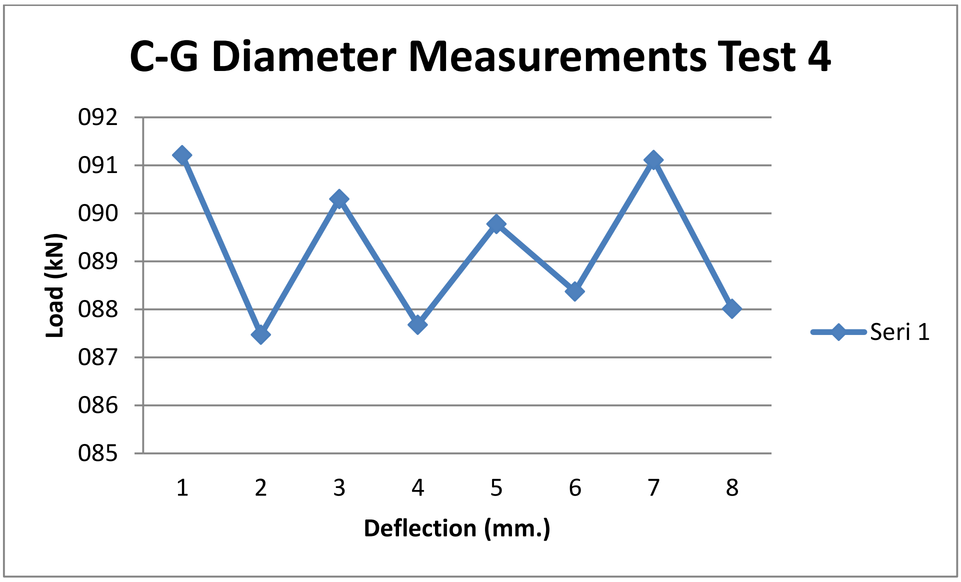

Figure 41 Measurement Data After 4. Test

After reaching the yield point it is also observed that in plastic region the toroidal shell behaves the same way as it can be seen on figure 40. It follows the same trend and this is probably the stiffness change did not affect the toroidal shell's behaviour in plastic region. The toroidal shell's final top and side view can be seen at figure 42 and figure 43.

Figure 42 Toroidal Shell Top View

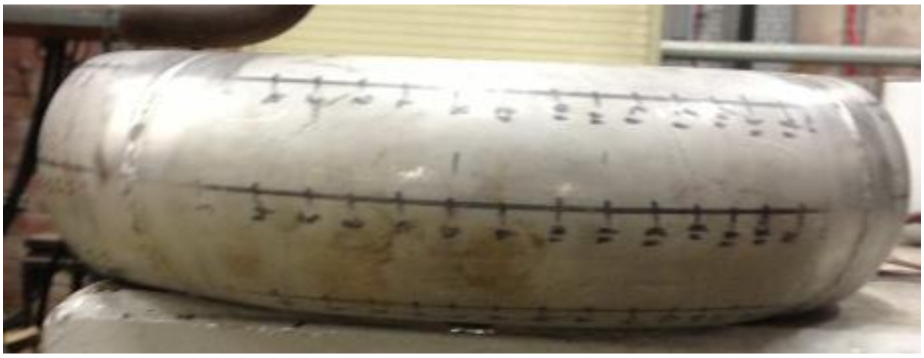

Figure 43 Toroidal Shell Side View

It has also been observed that the stiffness value did not change significantly on the forth test. The slope values for loadings have been given on table xx.

Table 7 Slope Values

	Test 1	Test 2	Test 3	Test 4
Slope	68,77	72,92	80,93	75,93

The values test 1, test 2 and test 3's values were calculated between the values of 20 and 60 kN for test 4 this value has been between 20 and 40 kN. The loading values were divided to 10 and an approximate slope has been calculated. The stiffness has been increased till test 3 but after test 3 the stiffness value has become more stable. The stiffness reduce on test 4 may be a result of, the defects. Valero et al.'s (2011) studies show that can vacancy defects can lower the stiffness values for long aligned-single walled carbon nanotubes. The defects may show the same effect for toroidal shell. Figure 44 shows an approximate combined test results.

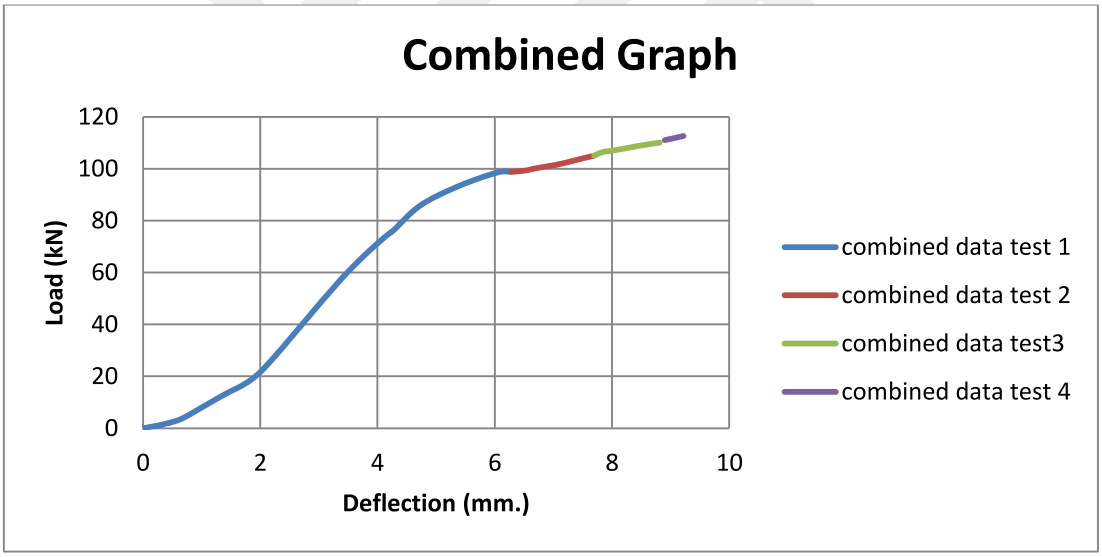

Figure 44 Combined Graph

In this graph the reason the deflection is higher before it reaches to 20 kN may be the toroidal shell's diameter is not the same value at every point, the contact area may be less before it reaches 20 kN. After the load reaches 20 kN the toroidal shell shows more stable deflection under the load change until it reaches around 80 kN. This may be the reason the load is applied more homogenously every point however this may not be the case for the loads below 20 kN. The yield point should be around 80 kN and the plastic deformation starts after this point. The deflection increases greater and the specimen become more sensitive to load change after it reaches the plastic region.

4. 2.Abaqus Results

The results of ABAQUS analysis is given below;

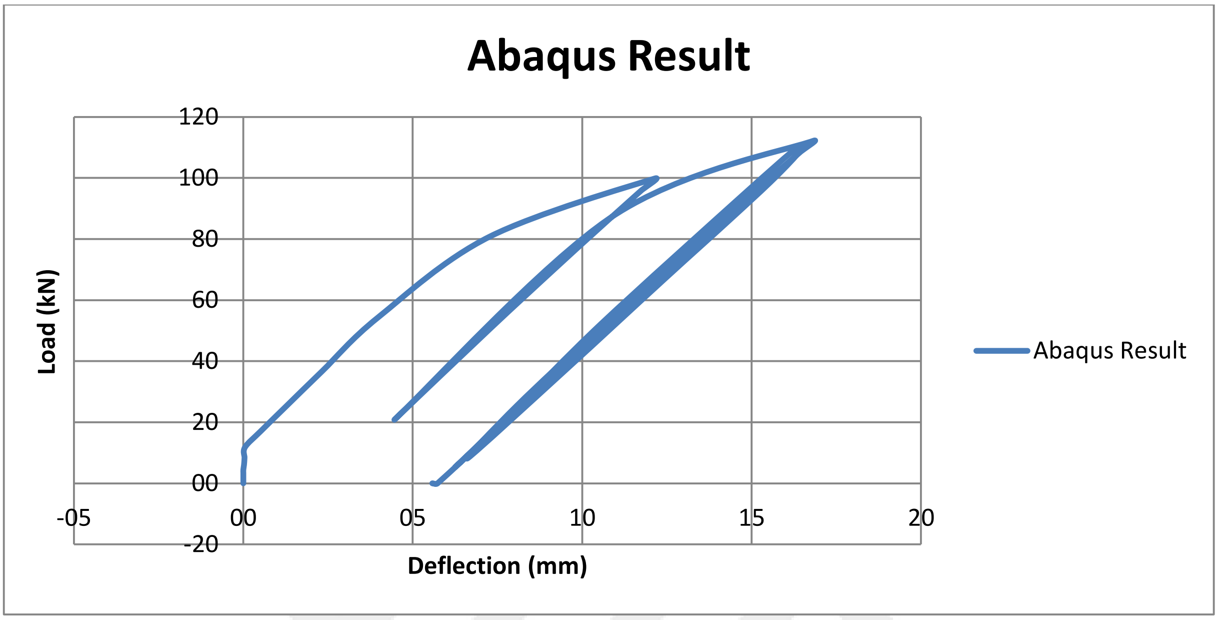

Figure 45Abaqus Results

The load is reaching a maximum 112.2 kN and the first loading is reaching to 99.8 kN the other tests could not be demonstrated because of modelling errors however, it can be seen that from this figure the loading profile in plastic region follows the same trend as it is observed at tests. The differences between tests and ABAQUS may be related with the assumptions, as ABAQUS model created as homogenous and the imperfections have not been modelled. The final model for ABAQUS result is shown at figure 46. The figure shows that the yield point for the toroidal shell is around 80 kN which is close to experiment values. As expected the second yield point after the second loading increases.

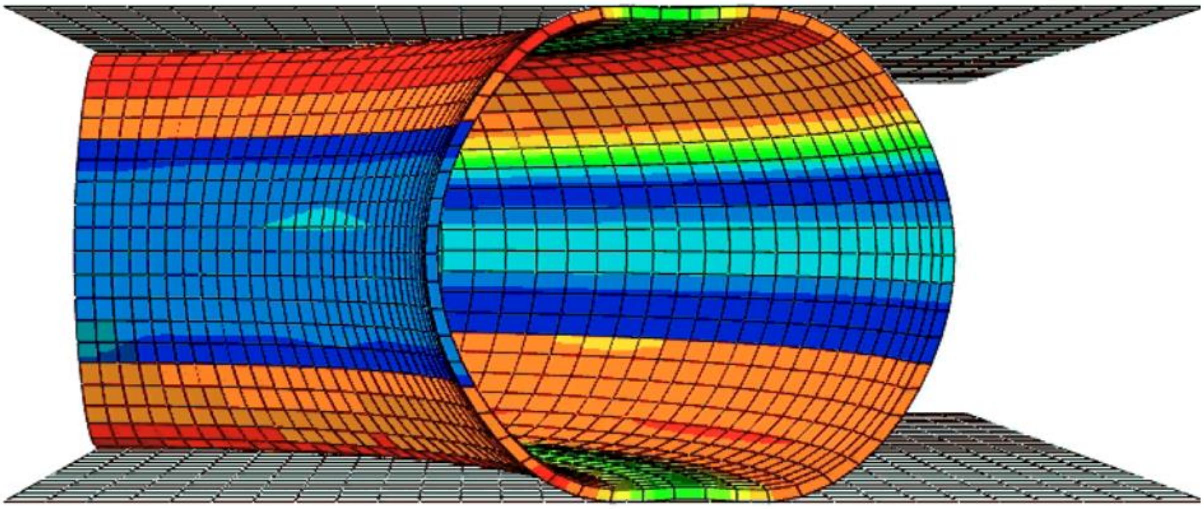

Figure 46 Final Shape Toroidal Shell

From the figure it can be seen that top parts gets flattened as expected but it also buckles in as the load increases therefore the contact area changes by time. The contact points are observed to have the highest von mises stress as expected. Simulation results show that as the contact area decreases the stress on contact area increases for similar loads.

5. Conclusion

5.1.Conclusion

The buckling of the toroidal shell has been analysed performing four different loadings and a computational simulation. Although at computational simulation results show that a concaving inside has been occurred, at experimental analysis this situation has not been observed. The loading and unloading procedure showed stiffness change due to density change and defects occurred on the specimen. To validate the accuracy of the results more experiments have to be performed to observe the behaviour on other toroidal shells, since only one specimen has been used. A more accurate ABAQUS model should be modelled observing all the loadings. It showed that ABAQUS model has not been reliable since the mesh density was limited due to the system limits the students to analyse the model on limited mesh density. Moreover, the analyser was not familiar with the ABAQUS software before and had limited time learning the software therefore; a more experienced ABAQUS software user may get more accurate results.

Although this research had reached its aims, there were some unavoidable limitations. First of all the research was conducted in 3 months if more time was given more data could have been collected to justify the significance of the analysis.

The research showed that the contact area on horizontal loadings change on different loads because the top surface flattens. Moreover, the toroidal shell may concave inside which also decreases the contact surface area.

5.2. Further Research

The horizontal loading for toroidal shell has been researched but more toroidal shells with the same geometry have to be tested to justify the significance of the results. To analyse the effect of the thickness of toroidal shells loadings for different thicknesses can be researched. For underwater submarine toroidal hull project, since the vertical loadings may be more important, also the vertical loadings have to be researched or a more realistic experimental environment can be created by conducting an experiment under high pressurised water in a pressure vessel.

For further research an ABAQUS analysis is required with higher mesh density and decreased time step to conduct more realistic simulation. To observe the effect of the manufacturing type other manufacturing types also has to be researched. An example to another manufacturing type can be creating a toroidal shell by welding two 180° elbows. For aerospace usage as a hull, the shells' behaviour has to observed on wind tunnels under different magnitudes of wind speed.

3.1. Work Plan

Gant chart of work plan is given below in the figure.

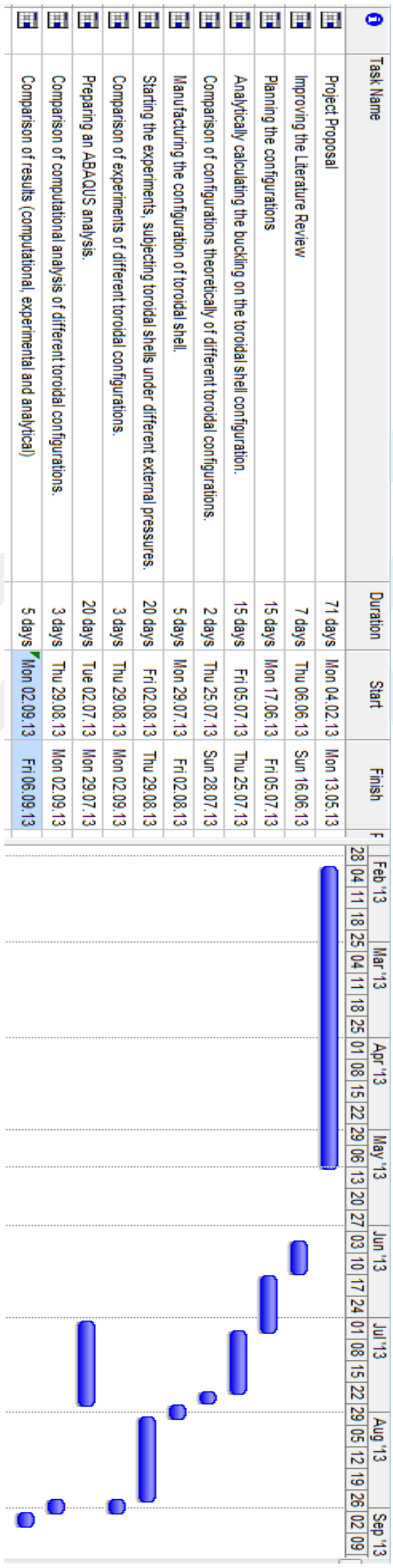

Figure 36 Gant chart of work plan

4. References

Blachut, J. (2004). Buckling and first ply failure of composite toroidal pressure hull, Computers and Structure, Vol. 82(1), pg 1981-1992

Baker, W., Bello, S.D., Marcuzzi, D., Sonato, P., Zaccaria, P. (2002). Design of a new toroidal shell and support structure, Fusion Engineering and Design, Vol. 63(1), pg. 461-466

Blachut, J., Jaiswal, O.R. (2000). On buckling of toroidal shells under external pressure, Computers and Structures, pg. 233-251

Crain, E.R. (ND). Calculating overburden pressure, from: http://www.spec2000.net/10-pressure.htm at:01.05.2013

Galletly , G.D. (1998). Elastic buckling of complete toroidal shells of elliptical cross-section subjected to uniform internal pressure, Thin-Walled Structures, Vol. 30(1), pg. 23-34

Galletly, G.D. (2000). Elastic buckling of externally-pressurized imperfect toroidal shells, International Journal of Structural Stability and Dynamics, Vol. 1(1), pg. 31-45

Hutchinson, J.W. (1967). Initial post-buckling behaviour of toroidal shell segments, Journal of Solid Structures, Vol. 3(1), pg. 97-115

Novozhilov, V., &Radok, J. (1959), The Theory Of Thin Shells [By] V.V. Novozhilov; Translated By P.G. Lowe; Edited By J.R.M. Radok, n.p.: Groningen: Noordhoff

Redekop, D., Xu, B., Zhang, Y.M. (1999). Stability of a toroidal fluid-containing shell, International Journal of Pressure Vessels and Piping, Vol 76(9), pg. 575-581

Ross, M. Buckling of toroidal shells under external pressures, [dissertation], University of Liverpool; 2013

Semenyuk, N.P., Zhukova, N.B. (2011). Stability of compound toroidal shells under external pressure, International Applied Mechanics, Vol. 47(5), pg. 545-553

Shikhirin, V.V. (2005). About tore technology and elastic engineering, from:http://www.elastoneering.com/abouttt.htm at: 01.05.2013

Skrzypek, J. (1990). Toroidal shell structures-governing equations and computerized analysis of curved tubes, elbows and bellows (a survey), MechanikaTeoretyczna, Vol. 28(1), pg. 217-242

Skrzypek, J., &Zyczkowski, M. (1983). Termination of processes of finite plastic deformations of incomplete toroidal shells, Solid Mechanics Arch., Vol. 8(1), pg. 39-98

Sun, B. (2010).Closed-form solution of axisymmetric slender elastic toroidal shells, J.Eng. Mech., Vol.136(10), pg. 1281-1288

Vu, V.T., Blachut, J. (2009). Plastic instability pressure of toroidal shells, Journal of Pressure Vessel Technology, Vol. 131 (5), pg. 512031-5120310

Wang, X.H., Redekop, D. Xu, B. (2006). FEM free vibration and buckling analysis of stiffened toroidal shells, Thin-Walled Structures, Vol. 44(1), pg. 2-9

Wie, B. and Bryson Jr., A.E. (1990). Transfer function analysis of a flexible toroidal structure, Journal Of Guidance, Control and Dynamics: A Publication Of the American Institute of Aeronautics and Astronautics Devoted to the Technology of Dynamics and Control,Vol. 13(5), pg. 881-886

Yasir, A.S. (2012). The cooling rate effect on the buckling strength and elastic properties of heated martensitic stainless steel columns, International Journal of Mechanical and Mechanics Engineering, Vol. 12(3), pg. 1-7

Zhan, H.J., Redekop, D. (2007). Vibration, buckling and collapse of ovaloid toroidal tanks, Thin-Walled Structures, Vol. 46, pg. 380-389

Zhan, H.J., Redekop, D. (2009). Static and dynamic loading of an ovaloid toroidal tank, Thin-Walled Structures, Vol. 47(1), pg. 760-767